1970

The adhesion of gold to single crystal alumina

L. L. Radke
Lehigh University

THE ADHESION OF GOLD TO SINGLE CRYSTAL ALUMINA

by

Leo L. Radke

A Thesis

Presented to the Graduate Committee

of Lehigh University

in Candidacy for the Degree of

Master of Science

in Metallurgy and Materials Science

Lehigh University

1970

CERTIFICATE OF APPROVAL

This thesis is accepted and approved in partial fulfillment of the requirements for the degree of Master of Science.

May 12, 1970
Date

Robert B Rumble
Professor in Charge

C. S. Canard Jr
Chairman of the Department
of Metallurgy and Materials
Science

ACKNOWLEDGEMENTS

The author expresses appreciation to Professor R. B. Runk of Lehigh University and to Dr. D. J. Shanefield of the Western Electric Company for their useful consultation and guidance in the preparation of this thesis.

The author is gratefully indebted to the Western Electric Company for sponsoring this work. The author expresses thanks to the following members of the staff at the Engineering Research Center: G. E. Crosby and M. J. Andrejco for occasional assistance, R. E. Mistler and J. A. Piazza for helpful discussions, F. Krainaker for construction of fixtures, W. H. Fisher for assistance in obtaining reference material, S. J. Buzash and B. S. Madsen for useful discussions of photomicroscopy and polishing techniques, and K. L. Morton for spectroscopic analysis of materials. The author expresses thanks to P. A. Renzo and S. MacNeil for preparation of the manuscript.

Above all, the author expresses grateful appreciation for the patience and understanding shown by his wife during the course of this project.

TABLE OF CONTENTS

LIST OF FIGURES

LIST OF TABLES

ABSTRACT

The adhesion of high purity gold to single crystal alumina has been investigated by use of the sessile drop method. An improved method for testing sessile drop adhesion couples is presented. The testing apparatus is capable of applying tensile loads in excess of 130 pounds. Minor amounts of oxygen in the ambient atmosphere during adhesion couple preparation are shown to have a strong influence on the bonding of this system. The maximum bond strength observed in this work was greater than 10,000 psi. A review of a proposed diffusion/van der Waal bonding model is presented which gives good predictions in some cases. The above model does not account for all of the observed adhesion characteristics for this system. An alternate bonding mechanism is proposed which is based on observations of the physical structure of the adhesion couple interface. This model assumes that an oxide of gold at the interface is responsible for the improved adhesion obtained from preparation in the presence of oxygen.

I INTRODUCTION

The fabrication of composite materials to meet specialized operational and environmental conditions has become a major part of modern manufacture. Thus the adhesion of the materials forming the composite is also of major importance. Accordingly, much work in materials research has centered on gaining a knowledge of adhesion mechanisms. From a detailed understanding of the adhesion mechanisms it is hoped that these fundamental principles can be used to predict the properties and characteristics of other potentially useful systems.

Thin films of gold on glass or high alumina substrates are becoming increasingly important in the electronics field. The full potential of such composites have not been realized due to the difficulties in obtaining satisfactory adherence of the gold films. It is the purpose of this paper to present a quantitive description of the adherence of gold sessile drops to single crystal alumina.

II LITERATURE REVIEW

In the broadest sense adhesion is a mechanical phenomenon. Its measure ultimately involves the response of the materials to a mechanical stress. Good adhesion in general requires contact on an atomic or molecular level. Obtaining contact at this scale is a necessary but not sufficient condition for good adherence. To develope such intimate contact between bulk materials, it is desirable to have one or both of the materials present in the liquid phase. This study is concerned primarily with the adhesion of a metal to a refactory oxide, thus only the metal will be in the liquid phase.

The interface formed by contacting two materials should have a lower surface free energy than the sum of the surface free energies of the separate materials. This is the Dupre reversible work concept. The Dupre equation for a liquid drop on a solid surface is

$$W_{AD} = F_{SV} + F_{LV} - F_{SL}$$

Where W_{AD} = work of adhesion

F_{SV} = surface free energy of the solid to the saturated vapor of the liquid

F_{LV} = surface free energy of the liquid to its saturated vapor

F_{SL} = surface free energy of the solid to the liquid

Surface tensions are dimensionally equivalent and under certain conditions numerically equal to the surface free energy per unit area, thus the relation is often written as

$$W_{AD} = \gamma_{SV} + \gamma_{LV} - \gamma_{SL}$$

The Dupre equation points out that work must be done to separate the materials, and equates this work to the negative of the reduction in surface free energy which occurs at the interface when the materials are placed in contact. The work of adhesion as here defined[13] is the work necessary to remove the liquid from the solid so as to leave an equilibrium vapor layer of the liquid on the solid. The Dupre relation is a logical and straightforward consequence from the consideration of free surfaces. The atoms in the surface layer of a material do not have the same coordination as an internal atom. As a result the surface atoms are in a higher energy state due to incomplete screening or shielding by adjacent atoms (unsatisfied valence state). If a second material is placed in intimate contact with the free surface it is possible that the atoms in the adjacent surfaces will interact to provide mutual screening and shielding with resultant decrease in energy. It is observed that this does not happen in all cases, e.g., an iron bar held for long times in a lead bath can be removed and there is no adherent lead film on the iron. This indicates that mutual solubility of the materials is a factor in adhesion. Iron and lead are essentially insoluble. Other factors

such as surface double layers can also influence the response of adjacent surfaces. If the surfaces have like surface charges a Coulombic repulsion force exists. Such properties are used to maintain a dispersion of colloidal particles in liquid suspension.

Consideration of the surface tensions acting at the perimeter of a liquid drop sitting on a flat smooth solid surface leads to Youngs equation

$$\gamma_{LV} \cos\phi = \gamma_{SV} - \gamma_{SL}$$

Where ϕ = contact angle measured internal to the liquid drop

This equation has been criticized in that it has no thermodynamic basis; however Lester[1] has shown it to be correct if the drop sits on a solid which is not too deformable. Combining the Young-Dupre relations results in

$$W_{AD} = \gamma_{LV} (1 + \cos\phi)$$

From which it is noted that the work of adhesion increases with decreasing contact angle. This implies that complete surface wetting ($\phi = 0$) is a requirement for the strongest bonding to occur; however Bondi[2] points out that even moderate wetting would be sufficient to form bonds stronger than the materials being bonded. If the system is cooled and solidification of the drop takes place such that there are no residual stresses in the interface, the Young-Dupre equation is assumed to remain valid for the bonded solids. This discussion[3] also assumes flat smooth surfaces, perfect contact, no intermediate phase

or defect at the interface, and equilibrium conditions after cooling.

The above assumptions are often far from valid in that the interface region can be highly stressed during cooling. This is caused by the unequal thermal expansion coefficients of the metal and oxide phases. Sutton[4] reports that some nickel alloys melted on sapphire to form a sessile drop develope sufficient residual stress across the interface during cooling to cause fracture of the underlying sapphire. The problems posed by residual stress in the interface region have motivated substantial development effort to find alloys with expansion coefficients similar to glass and/or ceramics. Alloys such as kovar and ceramvar have been developed to meet this need and are in extensive use for glass-metal or ceramic-metal seals.

The assumptions made for perfect contact and no defects in the interface are also seldom valid. Minor imperfections or irregularities in the interface can occur for numerous reasons such as small pits or scratches, a speck of dirt, local chemical action, or small patches which are not wet as well as the rest of the surface. Such defects can cause the nucleation and subsequent propagation of cracks. The magnitude of the effects these defects have on adherence is difficult to evaluate. The determination of true contact area is also very difficult if not impossible. Some workers[3] have suggested that compensating

terms be included in the expression for the work of adhesion; but these are of necessity no more than further assumptions to cover those cases where known residual stresses, imperfect contact, or interfacial defects exist.

The question of an intermediate phase in the interface is of critical importance. It has been reported[4] that small compositional changes in the metal have a marked effect on adherence. Composition gradients occur in the metal due to selective segregation of atoms to the interface or free surfaces[5,6]. The selective adsorption and segregation of solute atoms at the interface has been confirmed by x-ray fluoresence analysis. The species which gives the lowest surface free energy tends to gather at interfaces or free surfaces[7]. This is commonly observed in lead-tin solders. The surface is rich in lead, which has a lower surface free energy than tin. Small changes in environmental gases can cause significant changes in contact angles[3]. This is apparently caused by selective adsorption from the gas phase. The adsorbed gases are an intermediate phase in themselves and as such transform the adhesion problem into consideration of two interfaces[7] rather than one. An adsorbed layer of gas can prevent the desired intimate contact of the materials to be bonded, thus causing poor adherence. Mattox[8] has given an extensive discussion of the effects of these adsorbed gas layers. It is difficult to remove the adsorbed gases and equally hard to keep them off once

removed. Ultra high vacuum and high temperature are required to maintain an atomically clean surface for reasonably long times[9]. Paulson[10,24] has reported vapor deposition of gold films on glass which are highly adherent by use of ion bombardment for cleaning prior to deposition of a small amount of gold. After depositing the very thin layer (partial coverage only) a second ion bombardment cleaning was used followed by vapor deposition to form a layer approximately 2000 Å thick. The good adherence observed by Paulson is in sharp contrast to the very poor adherence of pure argon sputtered films[11] on such substrates. This example is a strong indication that a minor amount of adsorbed gas on the surface of the substrate can behave as an intermediate phase causing poor adherence.

The above discussion of the assumptions connected with the Young-Dupre equation are intended to point out that deviations from the theoretical predictions given by this equation should be expected. These deviations are caused primarily by the difficulties in achieving the conditions inherent to the theory. Furthermore this theory is based on energies, rather than the forces which are of more interest to the practical aspect of adhesion. Forces result from energy gradients and are directed from high to low energy states. The work of adhesion as here defined should therefore be considered as only a qualitative measure of adherence. For quantitive prediction of adhesion forces, or work of adhesion, a detailed knowledge

of the surface structures and types of bonds present across the interface is necessary. It is doubtful if such detailed knowledge of the surface structure can be obtained. Chang[22] has shown by use of LEED (low energy electron diffraction) that surface structures cannot be predicted from bulk single crystal orientation. The surface structure is also reported to take on different forms with temperature changes.

It should be noted that significant deviations from theoretical predictions for the strengths of materials are normally observed. These marked contrasts between theory and observed strengths have been related to various failure mechanisms. These mechanisms are activated at much lower stresses than are predicted from consideration of the elastic properties of materials only. The complications posed to the formulation of theoretical bonding models by such things as dislocation motion, crack formation, crack propagation, and work hardening are very serious. Consideration of these items has led some[12,13,23] to conclude that tensile or shear strength measurements of adhesion couples are of little value to support theoretical bonding models.

The various methods used to measure the adherence of materials also tends to yield only qualitative results. A prime example of this is the widely used scotch tape test for thin films suggested by Strong[26]. Shear[4,14] and tensile[20] tests have been used for sessile drop measurements and appear to be

reasonably good for materials that do not deform excessively during test. A variety of abrasion and scratch tests for thin films have been suggested. The scratch test described by Benjamin and Weaver[27], using a round ball to remove a clear channel in the film appears to be the most promising. This test is also somewhat limited in that detection of the clear channel is better suited to transparent materials. A direct attachment to films using glue, epoxy, or solder has been used but this method[28,29] has problems due to stresses introduced into the test specimen. Beams et al.,[32,33,34] have used an ultra-centrifuge apparatus to measure the tensile strength of thin films. By sectioning the film into discrete segments (areas) it is possible to measure the adhesion of the film to the rotor. The centrifuge method appears to be relatively error free but places restrictions on the materials which can be tested. The high accelerations available from ultrasonic transducers have also been used in adhesion studies[30,31]; however this method is rather indirect, and complex and has not found wide usage.

The measured strength values are also dependent on the process used to prepare the adhesion couples; e.g., vapor deposition, sputtering, electroplating, diffusion bonding, sessile drop technique, etc. The observed adhesion being dependent on the measuring procedure and fabrication process

tends to describe the "how" of adhesion rather than the "why". The causes of adhesion are related to the more fundamental physio-chemical properties of the materials and their environment.

Despite the problems noted above there are several recognized types of bonding that occur to produce good adherence between a metal and an oxide. These are chemical bonding to the surface oxygen anions[3,15,24], oxide formation on the metal phase with or without subsequent diffusion into the oxide phase to form a transition layer[14-18], psuedo-diffusion transition layer formed by high energy ion plating[8,11], van der Waal bonding[13,18,20,21,23] and a mechanically rough surface to provide an interlocking of the materials. Each of the major bond types are discussed further below.

The surfaces of oxides are dominated by the large oxygen anions[5], hence chemical bond formation is a distinct possibility for metals such as chromium, silicon, tantalum, etc. For these oxygen active metals a direct chemical bond (such as occurs in chemisorption)[15] to the surface oxygen anions is believed to occur. Gold films with underlayers of oxygen active metals have been studied and show very good initial adherence. In one study it was found that the adherence of these gold films decreased during aging[19]. For all cases studied, except chromium underlayers, the gold films are reported as being easily removed after aging in ambient room temperature atmosphere.

A thicker underlayer of oxygen active metal is also partially successful but causes other problems such as etching difficulties and are therefore generally undesirable.

Perhaps the best known example of the transition layer bonding is the Mo-Mn metalizing process for ceramics.[17] In this system a controlled partial pressure of oxygen is added to the system to oxidize the metal and form the transition layer. This process results in a metalized layer on the ceramic. An electroplate of copper or nickel is added and the part is ready for conventional solder joining to other parts. Benjamin and Weaver[15,16] report that iron films vapor deposited in a residual air atmosphere (10^{-3} to 10^{-5} torr) show a strength increase with age. It is concluded that trapped gas in the film (oxygen) diffuses to the interface to form a transition layer of iron oxide. Mattox[11] reports that argon-oxygen mixtures used as a sputtering gas to deposit gold films on glass produces highly adherent films. There was no claim made for the formation of a gold oxide transition layer but it is a plausible explanation since pure argon sputtered gold films are virtually nonadherent. Moore and Thornton[14] have melted gold on glass in oxygen to form sessile drops. Increased adherence for this processing is attributed to the formation of a gold oxide and its subsequent diffusion into the glass. An effort to verify this was made by use of radioactive gold tracers and appears to

confirm that gold diffusion into the glass does occur.

The psuedo-diffusion transition layer discussed by Mattox[8,11] is formed by high energy ion plating. During the initial period of deposition the impinging metal ions actually penetrate into the substrate thereby assuring that intimate contact is achieved. This technique could presumably be used to make strong composites from normally nonadherent materials. An addition to this concept to include charged particle ballistics control would enable "printing" of the desired shapes and patterns during deposition.

The van der Waal dispersion forces proposed by London have been receiving greater emphasis in theoretical adhesion studies[13,18,20,21,23]. The adhesion forces calculated from the proposed equations are admittedly a rough approximation[25], but such forces are much greater than the observed strength of most common materials. It has been pointed out that these dispersion forces are operative over greater distances than other bonding forces. When materials are in sufficiently close proximity for the formation of a chemical bond to occur, the actual formation of the chemical bond is irrelevant because the dispersion force acting through an even larger separation would alone exceed the strength of the joined materials.[13] The stability of the dispersion force bond to environmental and thermal treatments would probably not be as good, but these

are once again processing factors rather than fundamental causes of adhesion. Brandner[20] has proposed an oxide diffusion model combined with dispersion force bonding of gold to sapphire. He has shown a surprisingly good correlation of the diffusion activation energy as obtained from the model vs the so called extrinsic activation energy for oxygen self-diffusion in sapphire reported by Oishi and Kingery[35].

In summary of the previous discussion it is apparent that adhesion is a complex phenomenon. At this time there are three generally recognized causes or theoretical types of adhesion. These are[13], the adsorption theory, the diffusion theory, and the electrostatic theory.

III EXPERIMENTAL PROCEDURE

The gold-sapphire system inherently provides many desirable characteristics for a study of adhesion phenomenon. These materials are readily available in high purity forms, thus reducing complications caused by additional phases which could precipitate at the adhesion couple interface. Both of these materials are relatively chemically inert, further reducing contamination problems. This allows sample preparation in a variety of gas atmospheres. Since single crystal sapphire is transparent, the interface can be studied and photographed prior to testing the samples. Substrate grain boundary effects are also eliminated by use of the single crystal alumina. The thermal expansion properties are not well matched but gold has a low yield strength (500 psi), and thus a slow cooled sample should not have an appreciable stress at the interface.

Preparation of Materials

The sapphire discs were cut from a single crystal rod 5.2 inches long and 0.25 inches in diameter. The rod was obtained from the Adolph Meller Co., Providence, R.I. The listing in Table 1 indicates types and amount of impurity found by spectrographic analysis of the sapphire. The crystalographic orientation of the c axis relative to the rod axis was determined with the x-ray back reflection Laue technique. The rod was

TABLE I

Spectrographic Analysis of Materials

	I	II	III	IV	V	VI	VII	VIII
Sapphire	Al					Mg Ca		Si Fe
Gold	Au					Mg	Fe Ca	Si Cu Ti

Table 1 is a relative scale based on spectral line intensities. The indices I--VII represent decreasing concentration classes. Elements within a class are present in comparable amounts.

Elements checked for but not detected

Cd	Pb	Ge	V
Zn	W	Be	Cr
In	Sb	Zr	B
Mo	Sn	Bi	Ag
Co	As	Ga	Pt
		Na	Pd

mounted in a square steel bar with epoxy cement. This assembly was cut into slices approximately 0.375 inches thick. Each slice was further processed by grinding a flat on one side. See Figure 1 for details of the cutting geometry. The above procedure resulted in a disc with a wedge profile, which could be placed in a special holding jig for subsequent polishing and tensile tests. The discs were removed from the metal slice, cleaned in warm sulphuric acid, and numbered with a diamond tipped stylus. The numbering facilitated polishing operations, and served as a general reference for possible trends in adhesion data associated with a particular disc. The bottom edges of the discs were beveled to reduce stress concentrations and disc fracture in this area during tensile testing.

The discs were polished in groups, and from number identification each could be returned to the same position in the polishing fixture. The samples were polished with a series of diamond grit wheels, starting at 45 micron and finishing with 3 micron diamond particles. The surface finish of the polished discs was measured with an Engis roughness meter and was found to be nominally 0.4 microinch CLA (center line average). This compares to 2.2 microinch CLA for very smooth small grain ceramic substrates, and 0.2 microinch CLA for a standard glass microscope slide. After completing measurements and tensile testing each group of adhesion couples, the sapphire discs were repolished

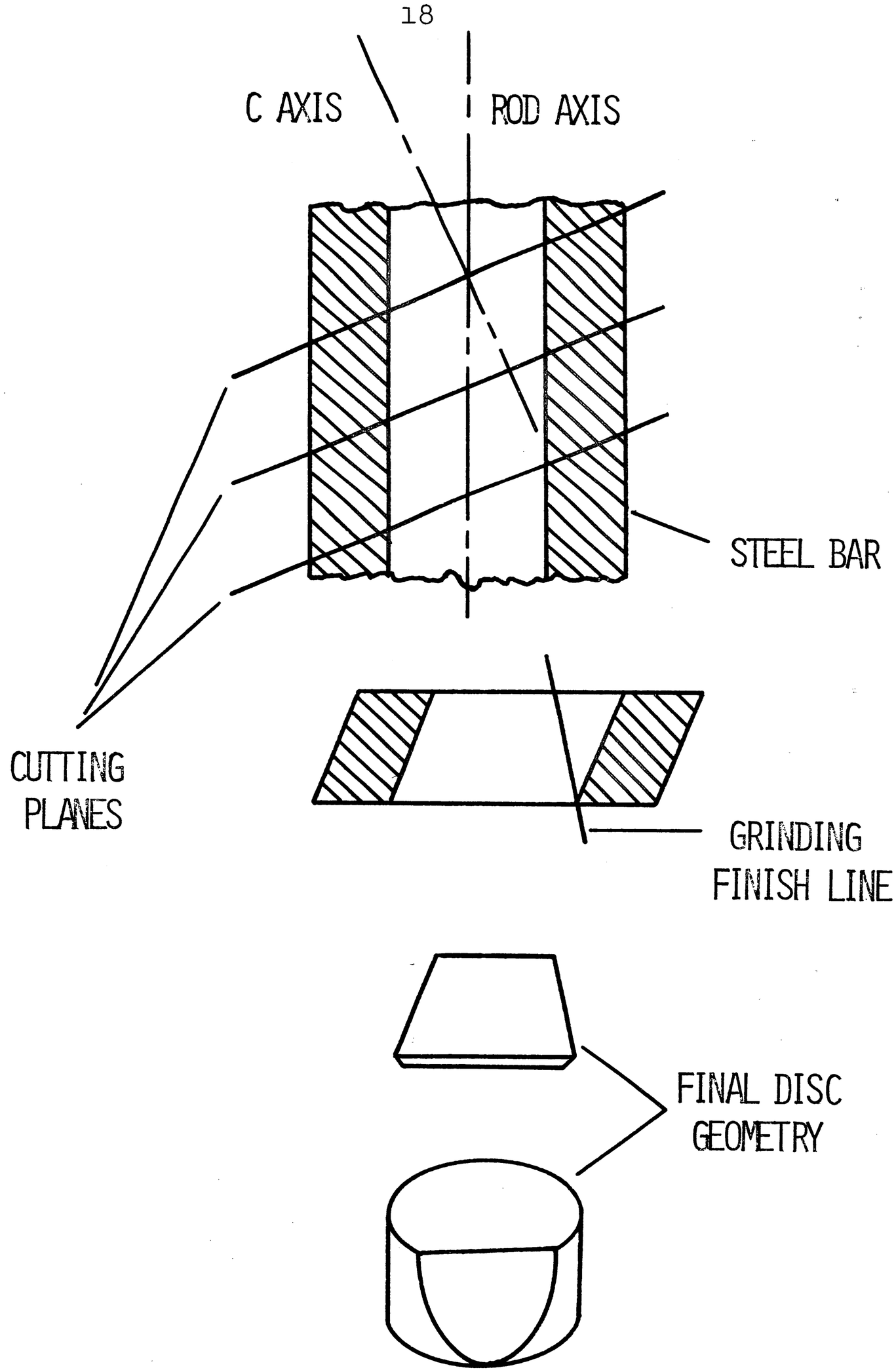

SAPPHIRE DISC SHAPING

FIGURE 1

prior to further use in subsequent tests.

Gold wire with a purity of 99.999 per cent was obtained from the Sigmund Cohn Corp., Mt. Vernon, N.Y. Table 1 also lists types and relative amount of impurities found by spectrographic analysis of the gold. The 0.040 inch diameter wire was cut into lengths with a sharp steel blade. The length of gold wire used in each series of couples was carefully controlled to check for possible wetting anomalies of the individual sapphire discs. In some of the series multiple lengths of wire were used. The wire was folded to form a boxlike shape and placed on the sapphire.

The cleaning procedure used to remove gross surface contaminations from the gold and sapphire samples is as follows; immerse in a mixture of equal parts hydrochloric acid and deionized water for 15 minutes, rinse in deionized water, ultrasonic washing in a proprietary cleaning solution (Aremco Corp. Crystalclean - 513) for 15 minutes, rinse in deionized water, rinse in denatured alcohol, and tumble dry on absorbent paper. The first group of samples (Run No. 1, Appendix I) were prepared by using a warm air stream for drying.[20] These samples did not have a smooth circular perimeter at the interface. This could have been caused by dust particle contamination during forced air drying. The warm air stream drying was not used for any subsequent work. Reduced contact angle, more circular area, and higher bond strength were noted in Run No. 2 and 3 for

otherwise equivalent processing.

Procedure for Adhesion Couple Processing

The adhesion couples were prepared by melting high purity gold on polished sapphire discs. The couples were made in an Englehart muffel tube furnace with a platinum heating coil. The furnace has a temperature range up to 1500° C. A check of the furnace temperature profile indicates a hot zone 3 inches long with a maximum variation of ±2° C. This furnace is suitable for use with various atmospheres in the heating tube such as oxygen, nitrogen, argon, or combinations of these. The heating tube (2.5 inch ID, 40 inches long) was made of high purity alumina material to reduce possible contamination during processing. Temperatures were monitored and recorded with a standard Barber-Coleman furnace controller. A Pt vs Pt/13%Rh thermocouple housed in a ceramic sleeve was used for temperature measurements.

The gold/sapphire samples were placed on a D tube and positioned in the hot zone. Moderately accurate leveling of the D tube and samples was necessary to prevent the liquid gold from rolling off or collecting at the edges of the discs. The furnace was preheated to 150° C prior to inserting the samples and introducing the selected gas environment. Heating was then continued at a nearly constant rate of 5° C per minute to the desired soak temperature. The environmental gases were metered

for flow control (3 to 5 liters per minute) and passed over a drying agent to reduce water vapor content. During later experiments when it was found that only minor amounts of oxygen appeared to have significant effects, the furnace was not pre-heated. The samples were loaded as usual and the furnace was flushed at 5 liters per minute with the desired atmosphere for 30 minutes. The flushing was continued for approximately one hour during the preheat cycle. After holding the samples at temperature for the desired soak time the furnace was cooled slowly (6° C per minute maximum) to 250° C or less before removing the samples from the furnace.

Two additional series of couples were made. One series was made in vacuum, 10^{-5} torr, by induction heating to melt the gold. Unfortunately this system introduced some contamination into the gold. The samples were made in a vacuum chamber normally used for pressure sintering ceramic powders. In this system a graphite susceptor forms a part of the pressure sintering mold. A new susceptor was used in this work; however it is believed that the contamination resulted from impurities in the susceptor. Some spalling and flaking of the susceptor material was noted. The other series of couples were made in a small experimental hydrogen furnace. After placing the samples in the furnace, a nitrogen purge was used to flush oxygen from the system. Dry hydrogen (-70° C dew point) was then introduced and ignited at

the furnace exit port with a glowbar burnoff device. The hydrogen flow was continued for 30 minutes prior to starting the heating cycle. The power input to the heating coil was manually controlled thus faster heating (15° C per minute) and cooling (10° C per minute) rates were used.

The gases normally used during sample processing were obtained from the gas distribution system in the research facility. As such, the gases are standard commercial grades. In later work special argon-oxygen mixtures were purchased in cylinders to enable more precise flowmetering for net oxygen content control. For example, a cylinder containing a 10 per cent oxygen--90 per cent argon gas mixture was combined with pure argon via flowmeters to yield a variable oxygen content mixture for use as the furnace atmosphere. The furnace pressure was one atmosphere in all cases.

Measurements and Testing

Measurements of drop geometry, contact angle, and interface area were made with a Jones and Lamson optical comparator and measuring machine (Model FC-14). All measurements and tracings of the interfacial area were made at a magnification of 31X. The tracings of the contact area were measured with a planimeter and converted to actual contact area. No attempt was made to correct for gas occlusions at the interface of the

samples. The larger gas occlusions were present to approximately the same degree in all samples as noted in viewing the interface through the sapphire at magnifications up to 100X.

Sessile drops of gold on sapphire have a contact angle greater than 110°. This geometry is suited to and suggests the use of a finger grip for tensile testing the adhesion couples. A grip as shown schematically in Figure 2 was made with four symmetrically spaced contact fingers. This is an improved version of the finger grip used by Brandner[20]. This grip is capable of applying tensile loads of up to 130 pounds (dependent on drop size) before slip and shear of the gold above the contact fingers takes place. The fingers of the grip assembly are forced against the sides of the sessile drop via a screw thread on the load support shaft. Small leaf springs in the body section push the fingers to the open position when the finger position control is raised.

In testing the stronger adhesion couples the grip fingers would sometimes slip and shear away a portion of the gold drop. A modified contact point as shown at the left proved to be more effective. The significance of the seemingly minor changes made in the tensile testing fixture were not realized immediately. During subsequent work it was found that the average strength for pure oxygen processed samples increased over 50 per cent as measured with the modified vs original grip fingers. The average

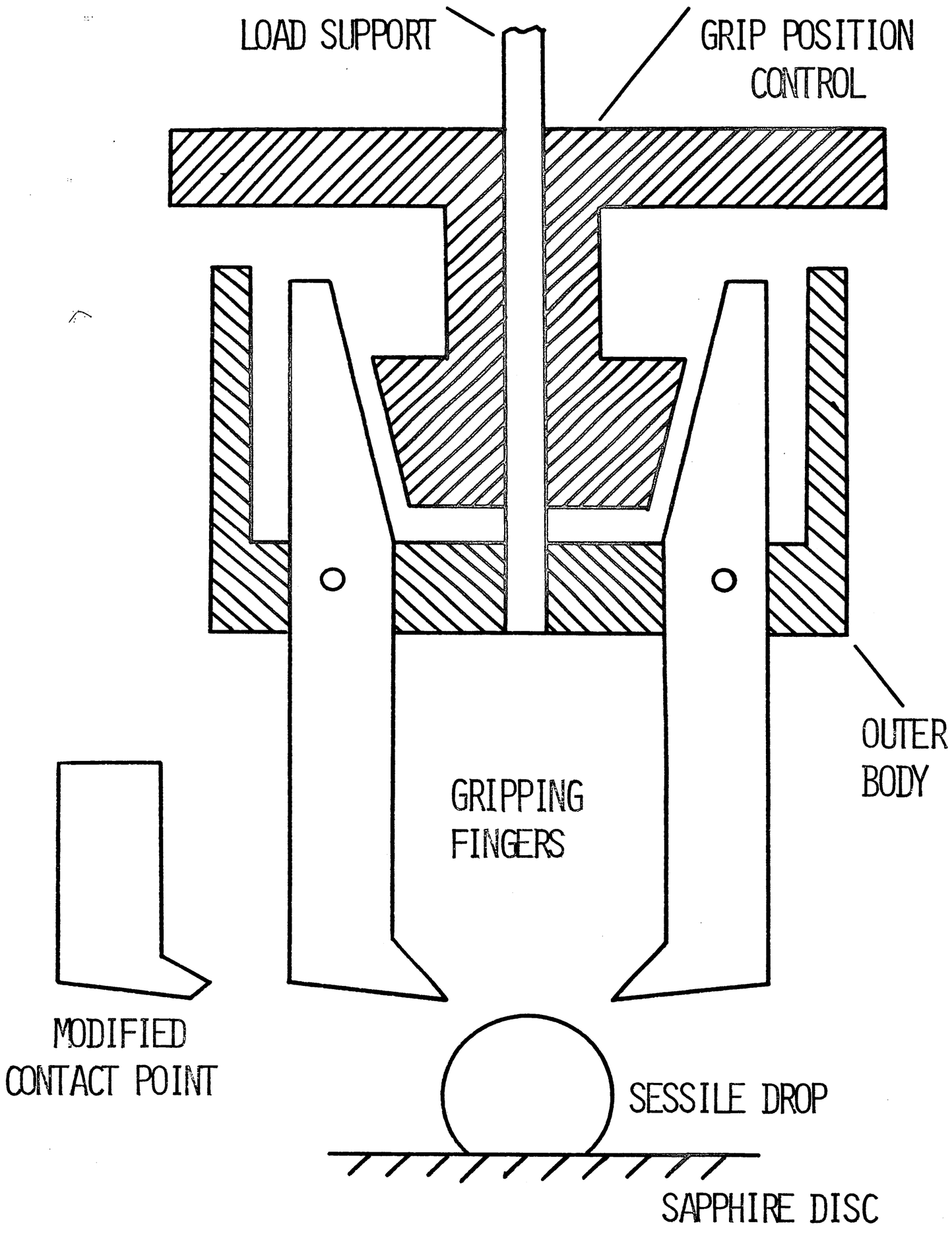

GRIP ASSEMBLY SCHEMATIC

FIGURE 2

strength for argon processed samples was the same for both arrangements. A completely satisfactory answer has not been found; however it is believed that the reverse slope on the bottom of the modified grip is partially responsible. The modified grip finger tends to dig into the drop, cutting through the surface, and thus transfers the load to the bulk of the drop. The original grip tends to rely more on friction with the outer surface. Since the outer surface of the drop is carrying a larger part of the load, peeling at the drop perimeter can occur resulting in a lower observed strength at failure.

The sapphire discs were mounted in a special holding fixture designed to assure that the interface remained horizontal and normal to the applied load. This was done to try to avoid interfacial shear stresses during tests. A simple dovetail slot arrangement does not meet this requirement unless the sessile drop is centered on the disc. The holding fixture is made in two sections as shown in Figure 3. The holder plate is drilled and leveled to mate with the sapphire disc. This part of the holder assembly is similar to the steel slice which results from the cutting/grinding operation as shown in Figure 1. The keeper plate is also beveled and shaped to match the holder plate. The keeper is placed on the holder and pinned in position. This results in an enclosure which contacts the

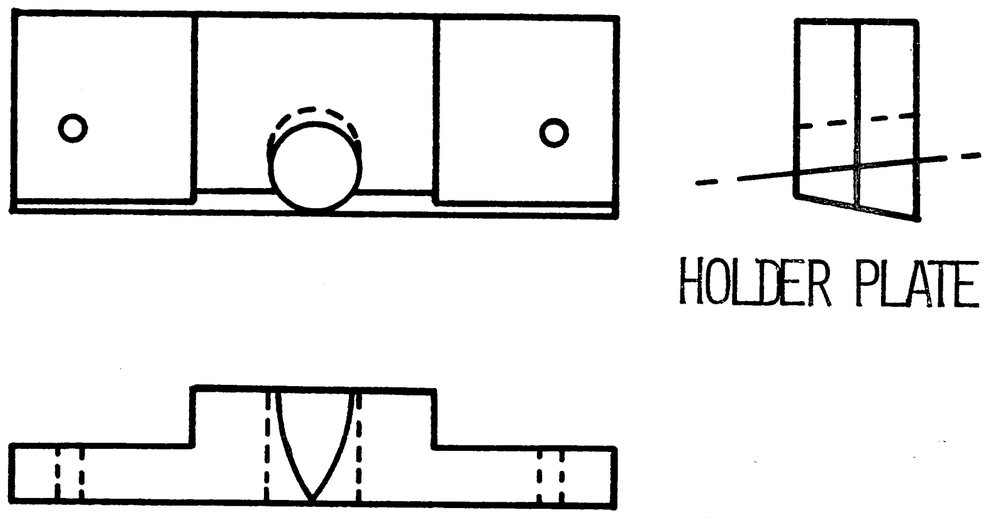

SAPPHIRE DISC HOLDER ASSEMBLY

FIGURE 3

entire periphery of the disc. The adhesion couples are inserted via the opening at the bottom but the wedge profile does not permit passage. Due to the small angles needed to expose the (0001) surface and maintain reasonable upper area on the disc, the compressive stresses in the sapphire are large as compared to the tensile stress at the interface. This compressive stress enhancement caused several samples to fracture at the bottom perimeter hence the need to bevel the discs at this point.

The adhesion couples were tested in an Instron testing machine. A crosshead speed of 0.1 inches per minute was used in all tests. The applied load at failure was obtained from a strip chart recorder plot for each sample tested. The strip chart was operated at a speed of 20 inches per minute to display more detail in the loading/fracture cycle. The stress level at failure was calculated from load/area measurements and tabulated in Appendix I. The listed value for the contact angle is obtained by taking an average of the values for the individual drops in that group. The data are arranged such that the first 13 groups of samples were tested with the original testing grip, all others were tested with the modified grip assembly.

IV EXPERIMENTAL RESULTS

It has been reported that the presence of oxygen causes an improved adherence of gold to glass[14] and alumina[20]. One of the primary goals of this work was to determine the effects of oxygen partial pressure on the adhesion of the gold-sapphire system. Data for further testing of a proposed bonding model[20] is also presented. The following sections present the results of tensile tests made on the adhesion couples. Observations of the physical characteristics of the interface area are also given.

1. Hydrogen Processed Couples

To obtain very low oxygen partial pressures, two groups of adhesion couples were prepared in a dry hydrogen atmosphere. By use of the hydrogen gas dew point data and the Richardson diagram, it is estimated that the partial pressure of oxygen in the furnace was well below 10^{-15} atmospheres. The furnace used to prepare these samples was equipped with a view port at one end. As the gold melted the formation of the sessile drops was observed. The wire frame initially collapsed onto the disc, and within 10 to 15 seconds the gold became sufficiently fluid to allow the surface tension forces to form the typical oblate spheroid shape.

The average tensile strength of these couples was 550 psi. The interface of all the samples contained gas occlusions, and many tiny occlusions in the form of negative crystals. The photomicrographs in Figure 4 are examples of the latter interfacial defects observed at the drop perimeter after tensile testing. In Figure 4A

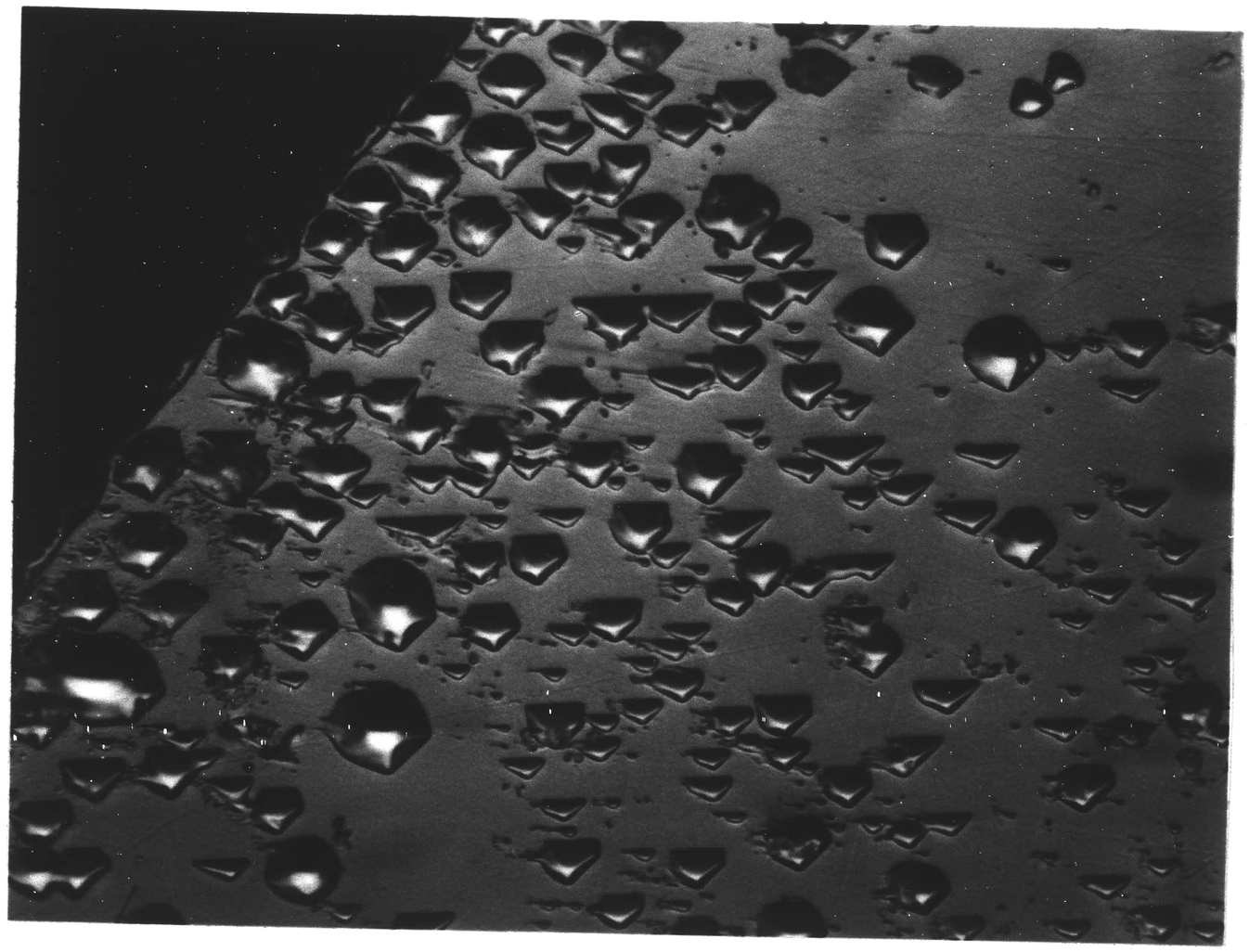

4A
500X

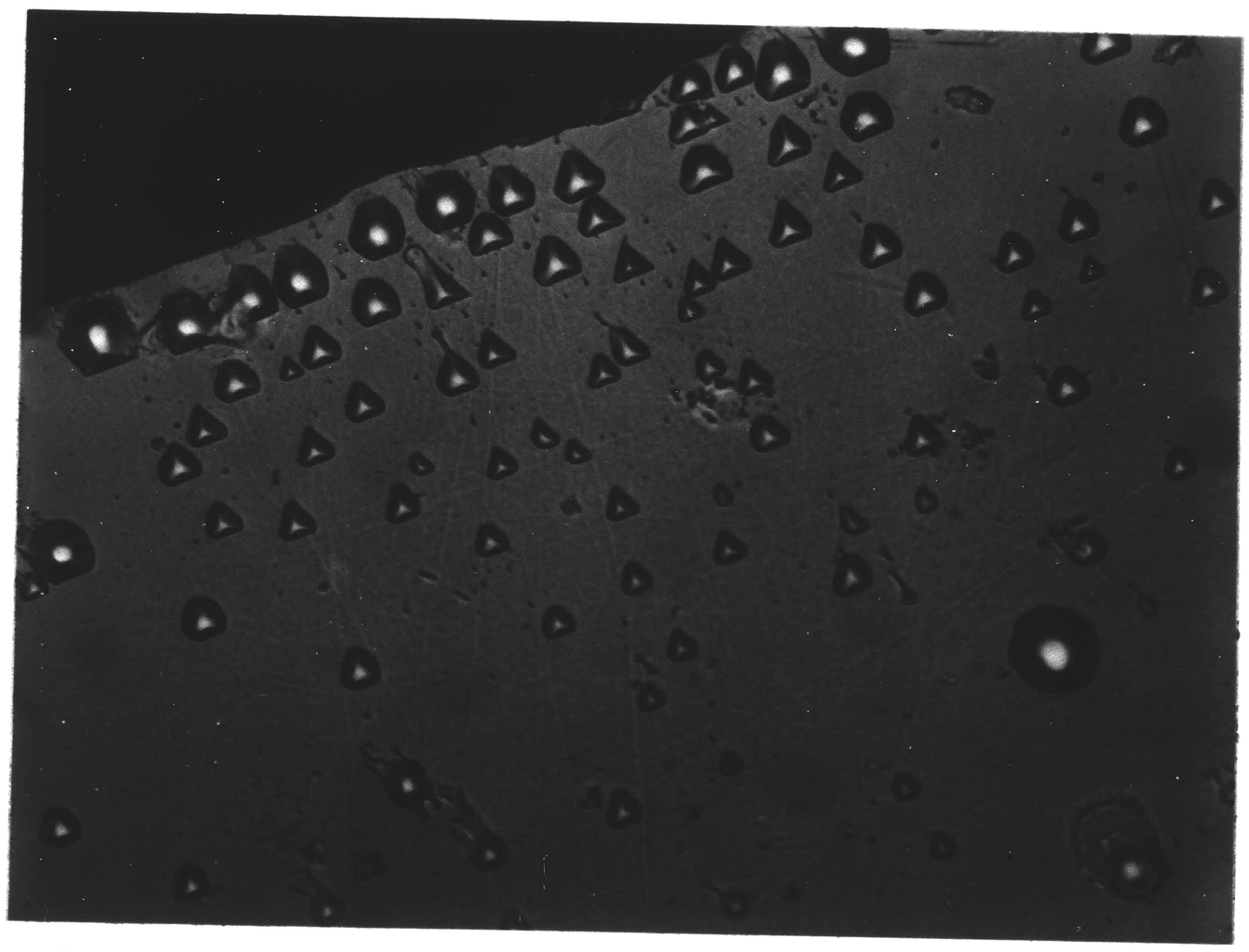

4B
500X

HYDROGEN PROCESSED GOLD

FIGURE 4

it is seen that many of these defects impinge upon one another. Hydrogen is known to be slightly soluble in liquid gold which suggests that the defects were produced by gas precipitation during cooling. The generally good resolution shown in Figure 4 is a direct result of the poor bonding. These samples did not deform significantly during tensile testing.

2. Argon Processed Couples

A series of adhesion couples were prepared in an argon atmosphere. The results of the tensile tests made on these samples are listed in Table 2. Detailed sample processing is also noted therein. The average stress at failure for the first three groups of samples is similar. This indicates a reasonably good reproducibility in the processing and testing of the samples. This is also noted for runs 2 and 3 of Table 5. The other data listed here result from intentional oxygen exposure, and from efforts to exclude oxygen and other gases from the furnace during sample preparation. An indication that not all foreign gases were removed from the furnace is shown in the photomicrographs in Figure 5. The structure of the gold surface shown in these photomicrographs is believed to result from gas expulsion from the gold during cooling. Figure 5A was obtained from an area adjacent to several larger gas occlusions. Figure 5B is an area at the drop perimeter showing substancially less defects and is more typical of these surfaces.

3. Argon-Oxygen Processed Couples

Atmospheres of mixed argon and oxygen were used to obtain data

TABLE 2

Argon Adhesion Data

Run No.	Notes	Time (hrs)	Ave. Stress (psi)
8	1	1:02	3286
9	1	1:08	3356
11	1	1:00	3445
21	2	1:08	3306
19	3	1:23	3002
20	3	1:00	2542

Notes:

1. Preheated furnace.

2. Heated to 500°C in oxygen, switched to argon atmosphere, flushed system, and continued heating cycle.

3. Furnace not preheated, argon flushed before heating cycle.

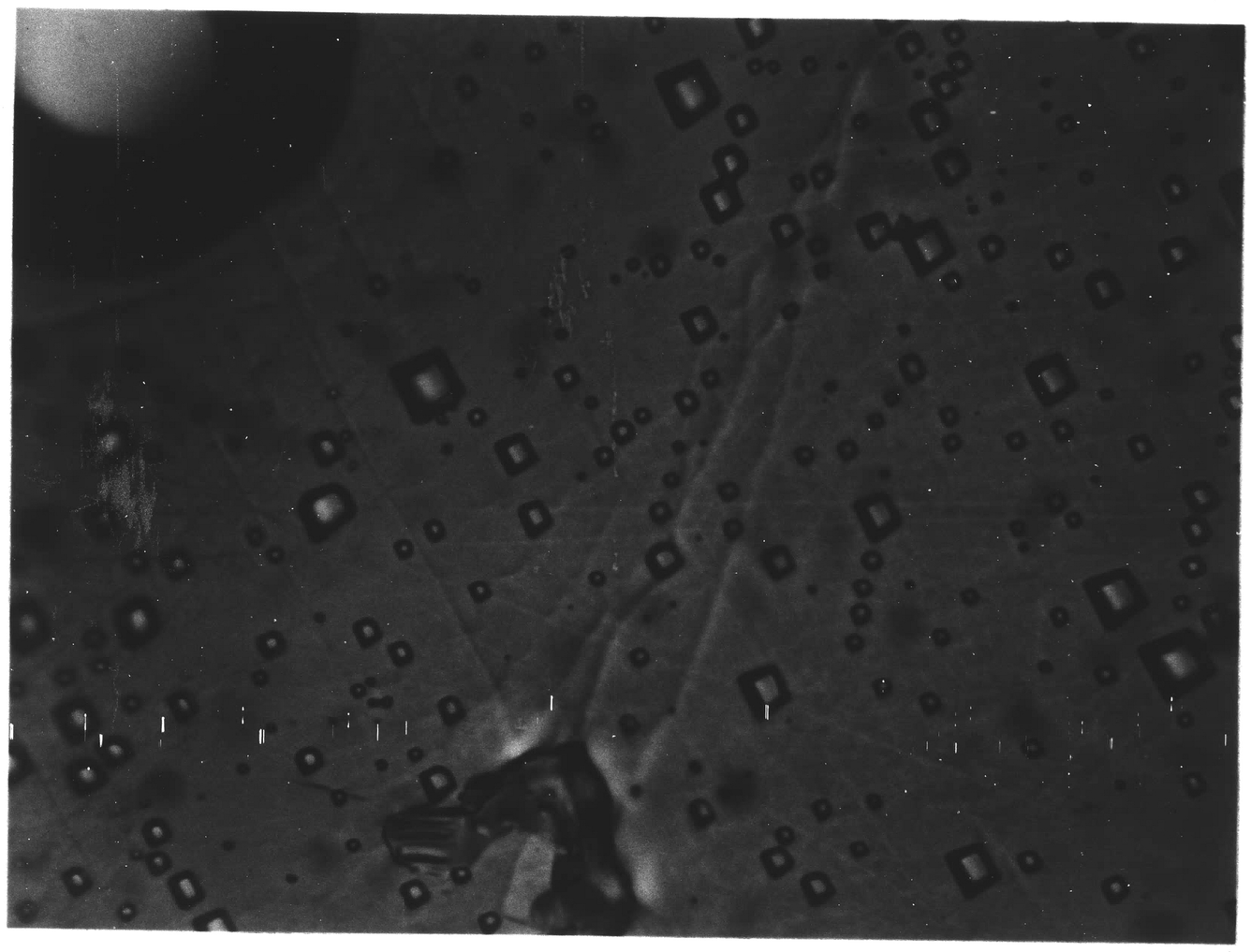

5A
1000X

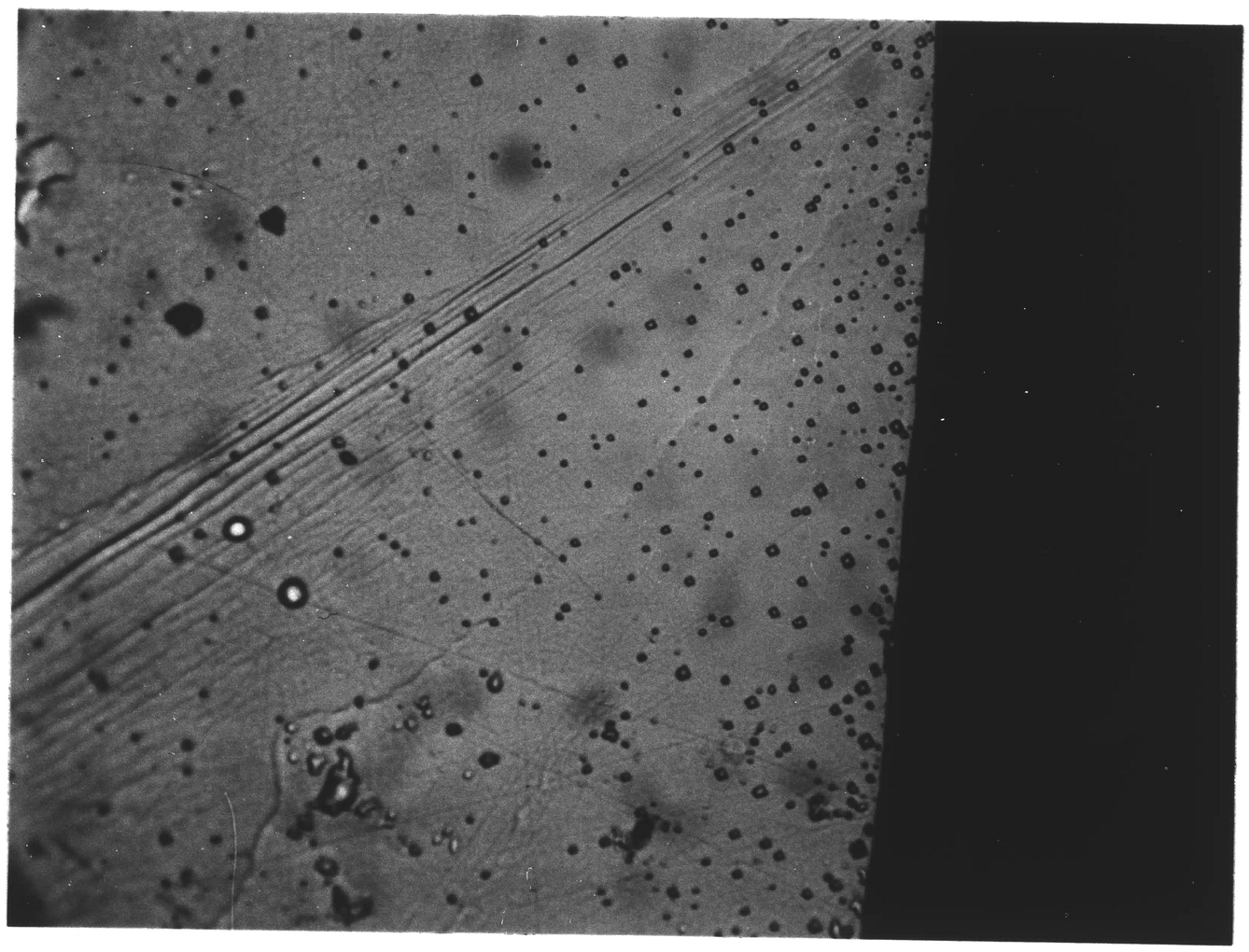

5B
500X

ARGON PROCESSED GOLD

FIGURE 5

at several additional values of oxygen partial pressure. The tensile strength data for these samples is listed in Table 3, and will be discussed in a later section.

An examination of the adhesion couple interface before and after tensile testing confirmed that minor sapphire particles are sometimes pulled out of the surface. The photomicrographs in Figure 6 show a flake of sapphire remaining on the gold, and the corresponding pullout area from the sapphire disc. The later photograph was taken with transmitted light to display more of the details of the fractured surface. The faint rings at the lower right are caused by gold remaining on the sapphire surface. Small rings of gold marking the position of interfacial gas occlusions were frequently noted when the samples were processed in the presence of oxygen. This disc was examined during subsequent polishing, and what appeared to be a small pit was found at one end of the pullout. It is believed that the pit results from fracture at an internal defect near the surface of the sapphire. Numerous internal defects such as shown in Figure 7 were found in the material. The hexagonal pattern expected for the (0001) plane of sapphire is clearly shown in one of the defects in Figure 7B.

4. Nitrogen-Oxygen Processed Couples

Several runs were made using mixed nitrogen-oxygen gas atmospheres. This was done to determine if nitrogen would have an adverse effect on the bond strength as compared to argon. The results of the tensile tests are listed in Table 4. The values are

TABLE 3

Argon-Oxygen Adhesion Data

Run No.	Time (hrs.)	Percent O_2	Ave. Stress (psi)
21	1:08	--	3306
28	1:05	2	5145
26	1:05	5	5224
27	1:08	10	5605
22	1:00	10	4875
23	1:04	20	5507
18	1:06	100	6439

6A
200X

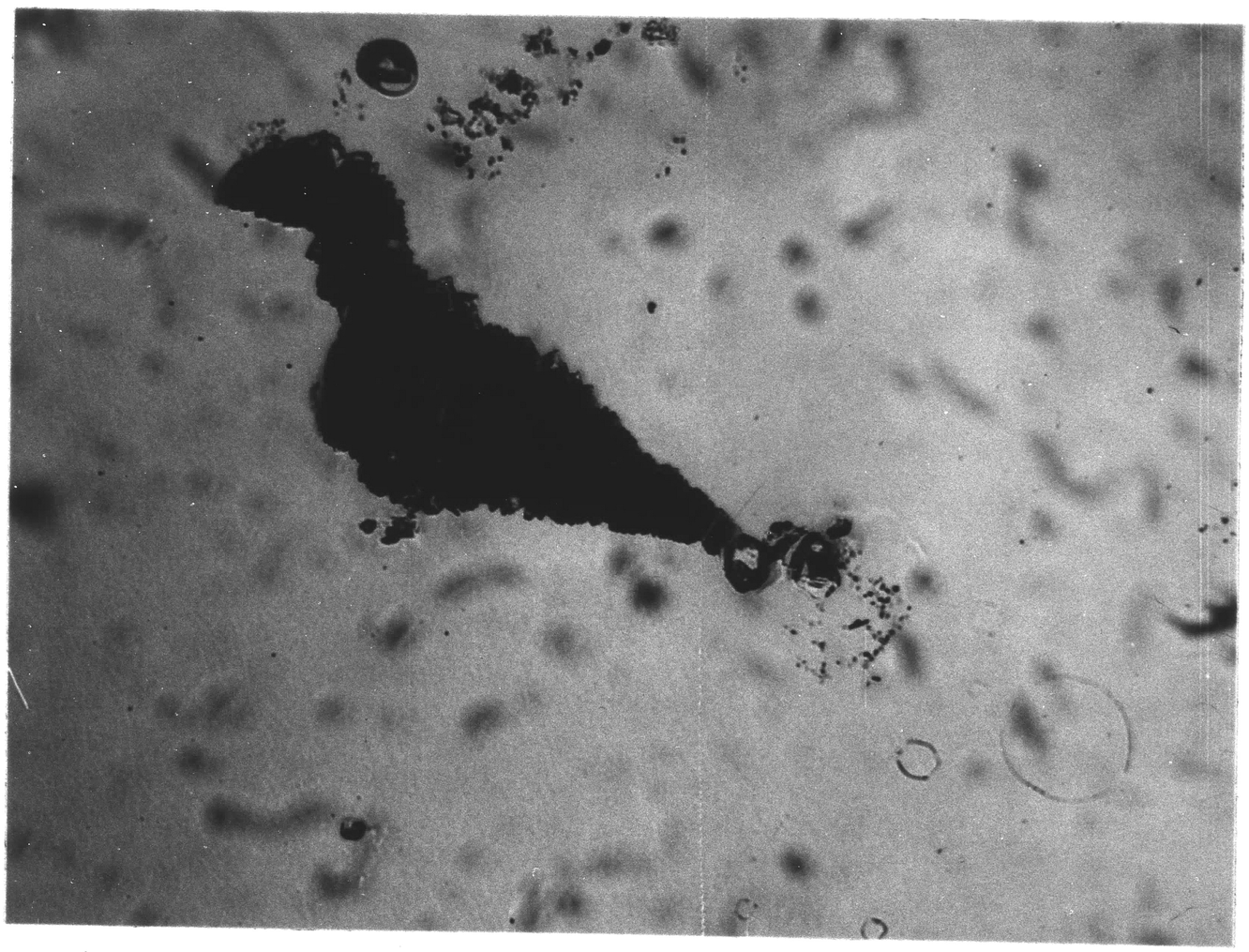

6B
200X

SAPPHIRE PULLOUT

FIGURE 6

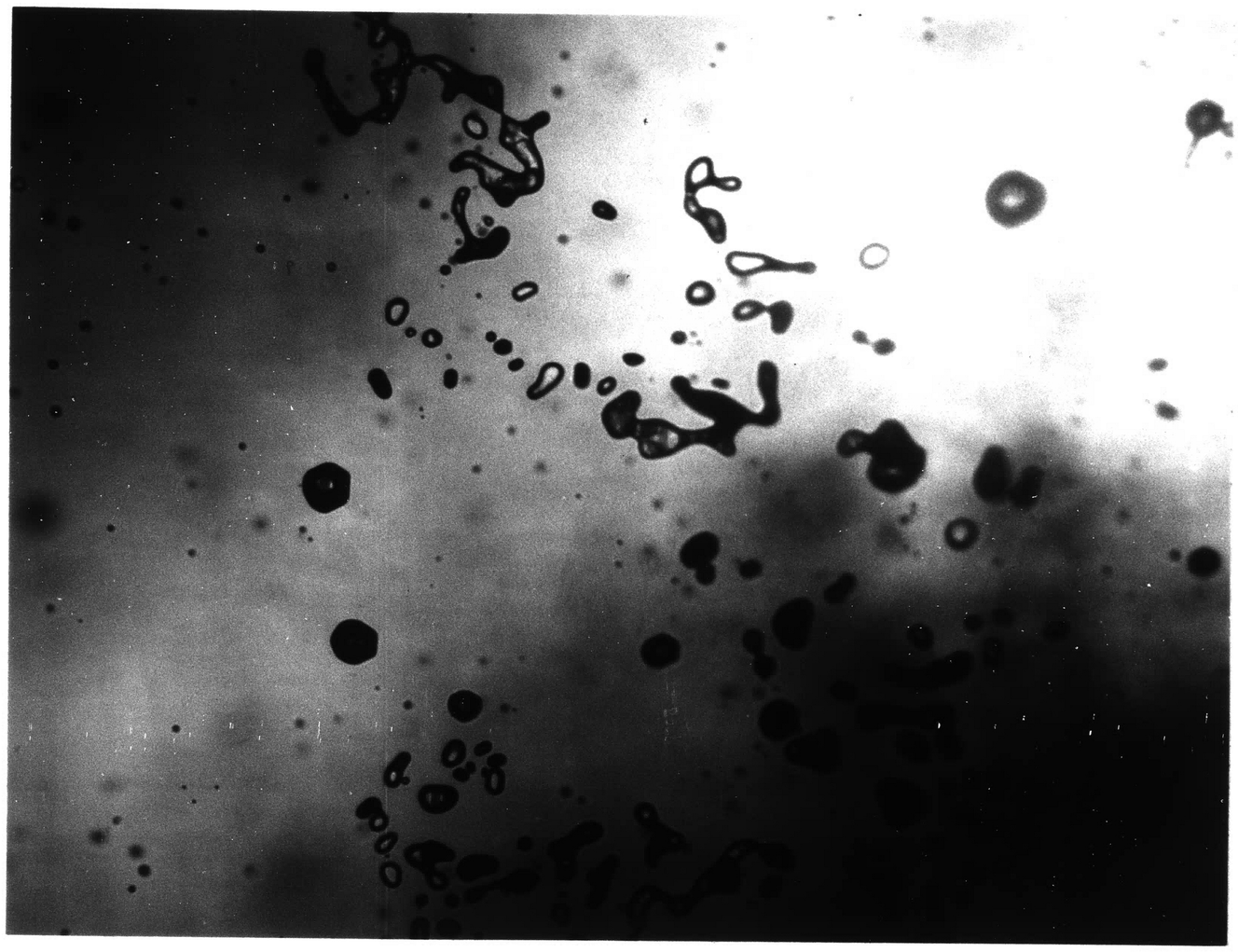

7A

100X

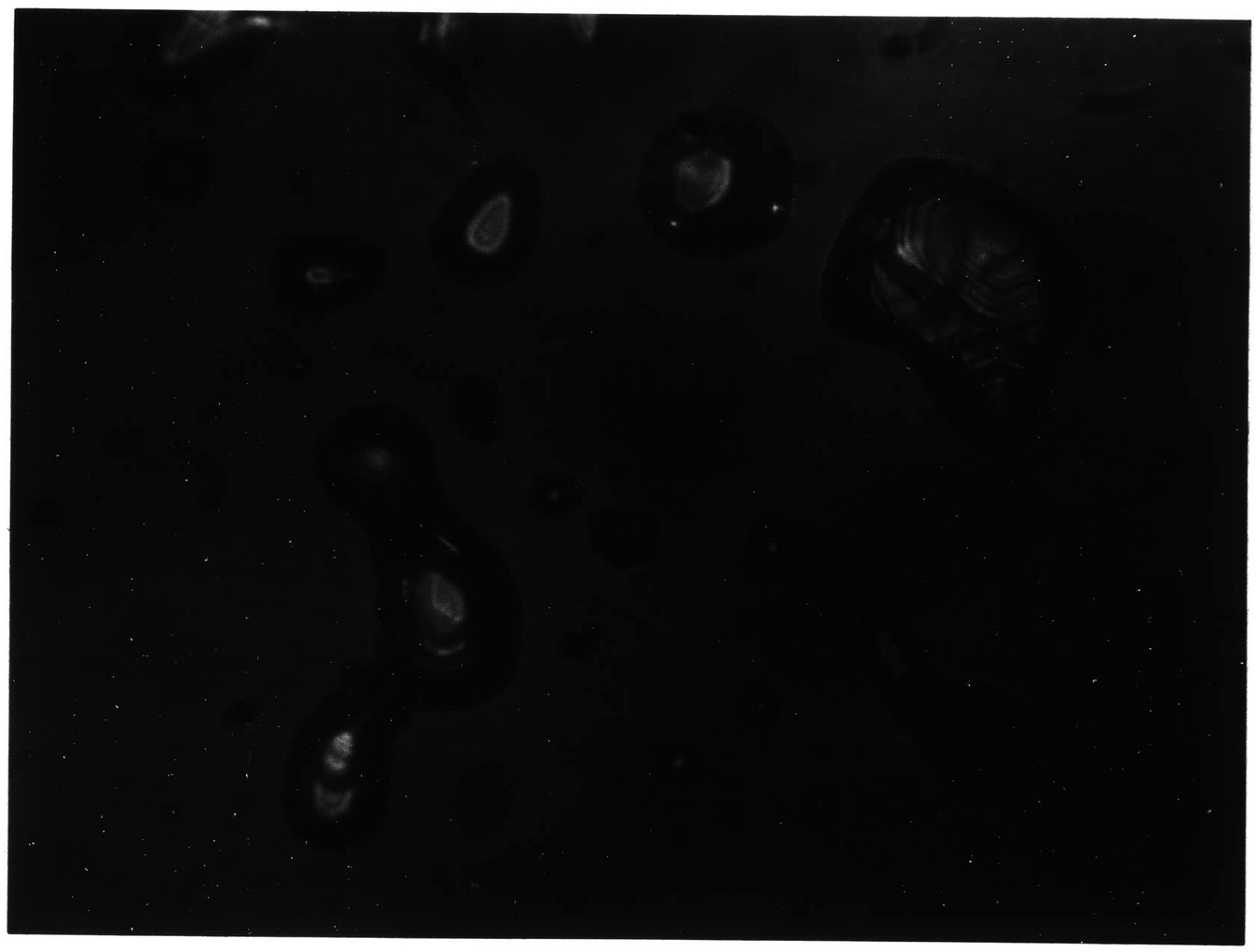

7B

500X

SAPPHIRE INTERNAL DEFECTS

FIGURE 7

TABLE 4

Nitrogen-Oxygen Adhesion Data

Run No.	Time (hrs.)	Percent O_2	Ave. Stress (psi)
17	1:18	--	3598
24	1:00	Air	5185
16	1:45	Air	5700
25	1:06	50	5272
18	1:06	100	6439

quite comparable to those listed in Table 3. The strength differences for pure nitrogen vs argon, and the differences in the two air runs can be attributed to the variation in time at high temperature. The bond strength time dependence is discussed further later.

Nitrogen is also known to be slightly soluble in liquid gold, and the occurrence of relatively large numbers of negative crystals was observed. Typical examples are shown in Figure 8. In Figure 8A the precipitation appears to have occurred along polish marks in the sapphire. In the two views of another sample shown in Figure 8B and 8C it is seen that some of these small occlusions have grown sufficiently to reach the perimeter of the drop.

5. Oxygen Processed Couples

A series of adhesion couples were made in an oxygen atmosphere by holding the samples at constant temperature for various times as shown in Table 5. These data are discussed later in an analysis of a proposed bonding model. Numerous examples of gold remaining on the surface of the sapphire discs were found. The photomicrograph in Figure 9A contains small rings marking the position of gas occlusions. The triangular areas in Figure 9B result from the negative crystals noted at the interface of some samples. The number of negative crystals noted in the interface increased for longer processing time.

The photomicrographs in Figure 10 show the effects of the stronger bonding obtained by oxygen processing. Slip lines and substancial distortion of the gold drop are shown in Figure 10A.

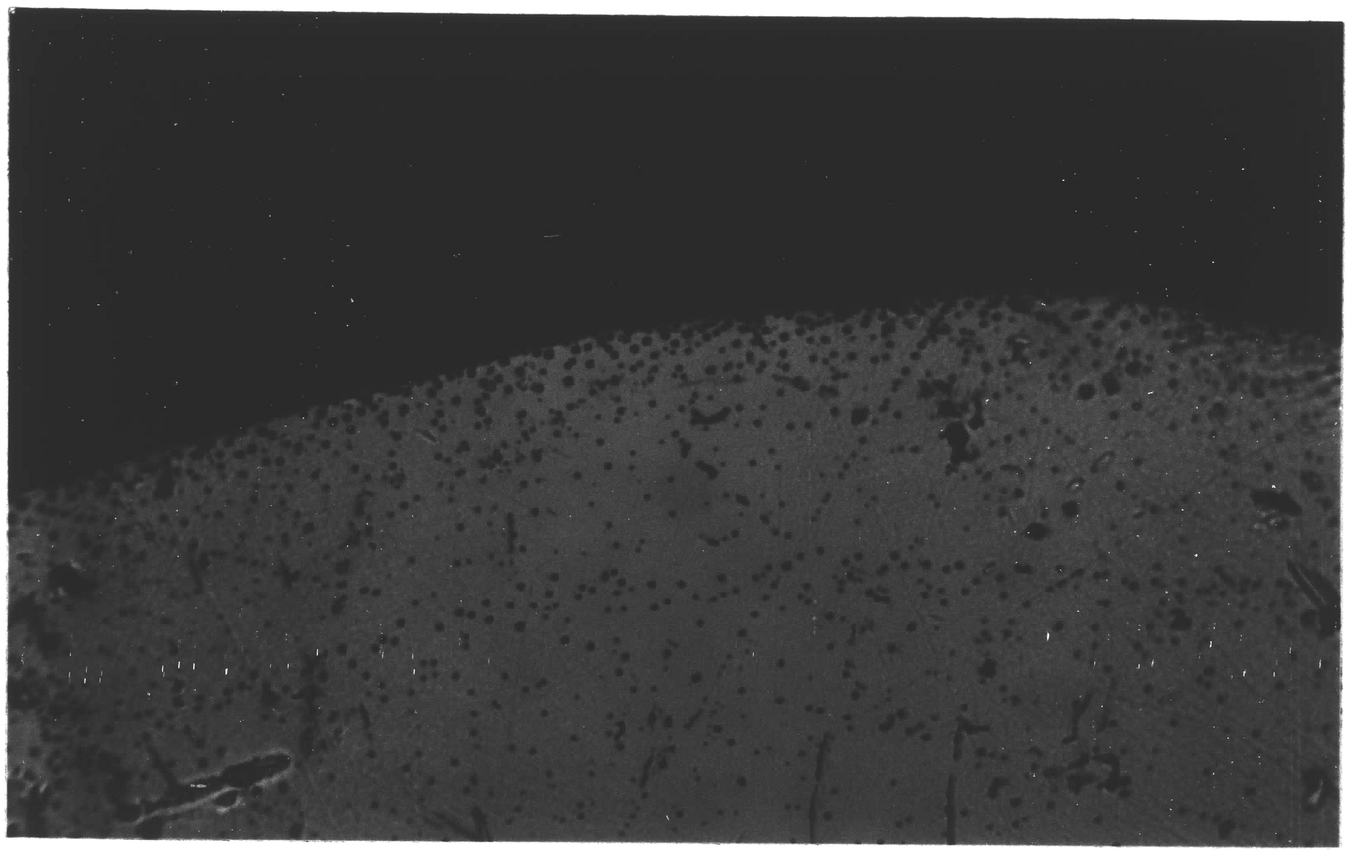

8A
200X

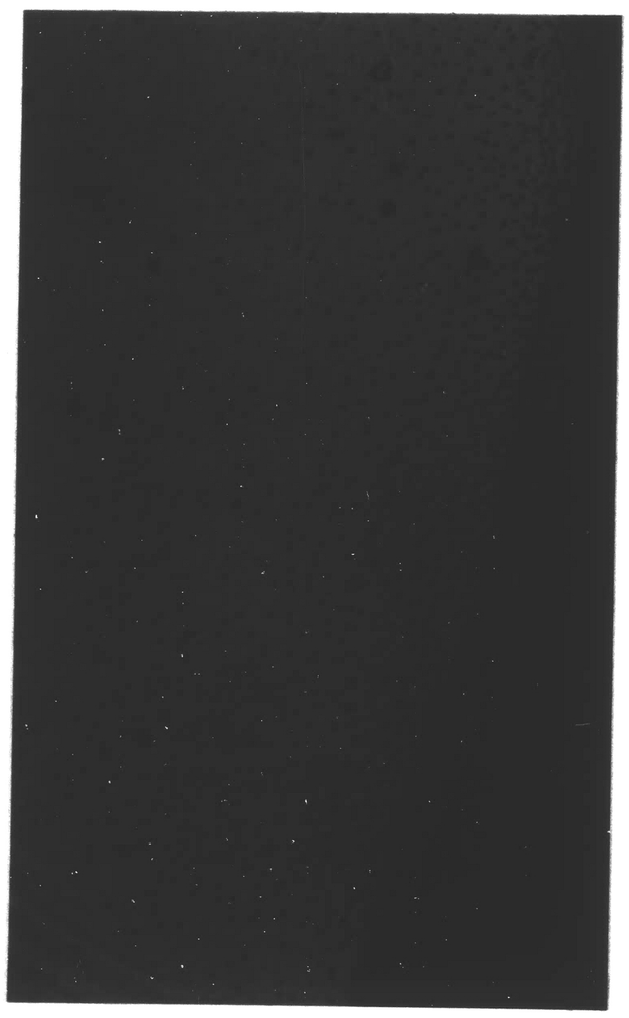

8B
200X

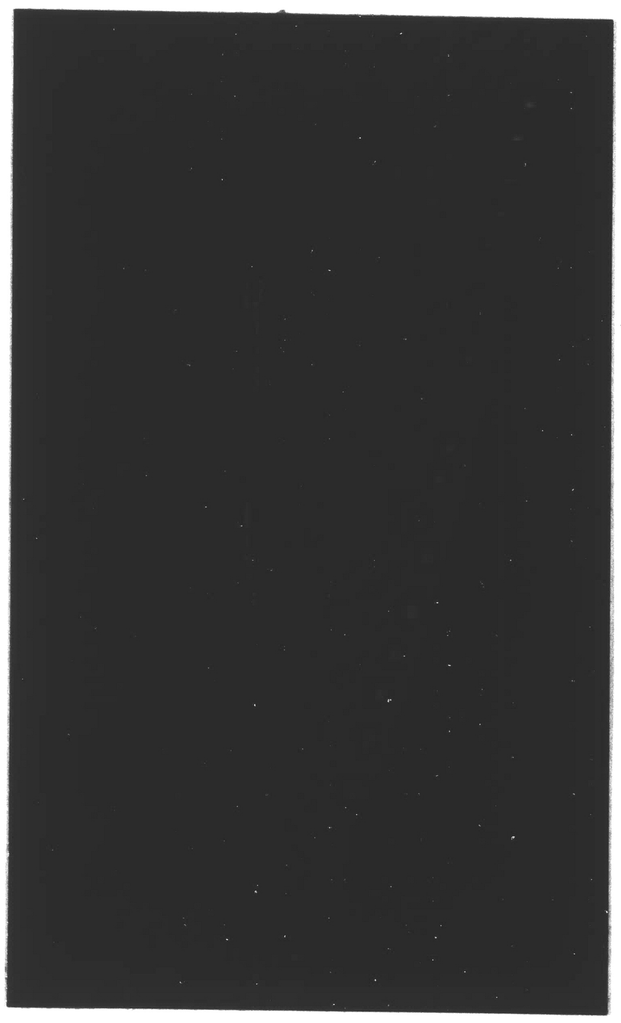

8C
500X

NITROGEN PROCESSED GOLD

FIGURE 8

TABLE 5

Oxygen Adhesion Data

Run No.	Time (hrs.)	Ave. Stress (psi)	Max. Stress (psi)
2	1:03	4079	4824
3	1:07	4046	5005
7	1:58	4290	5304
4	4:16	5019	5666
10	7:15	5469	6394
6	9:52	4275	5336
5	10:15	4687	6408

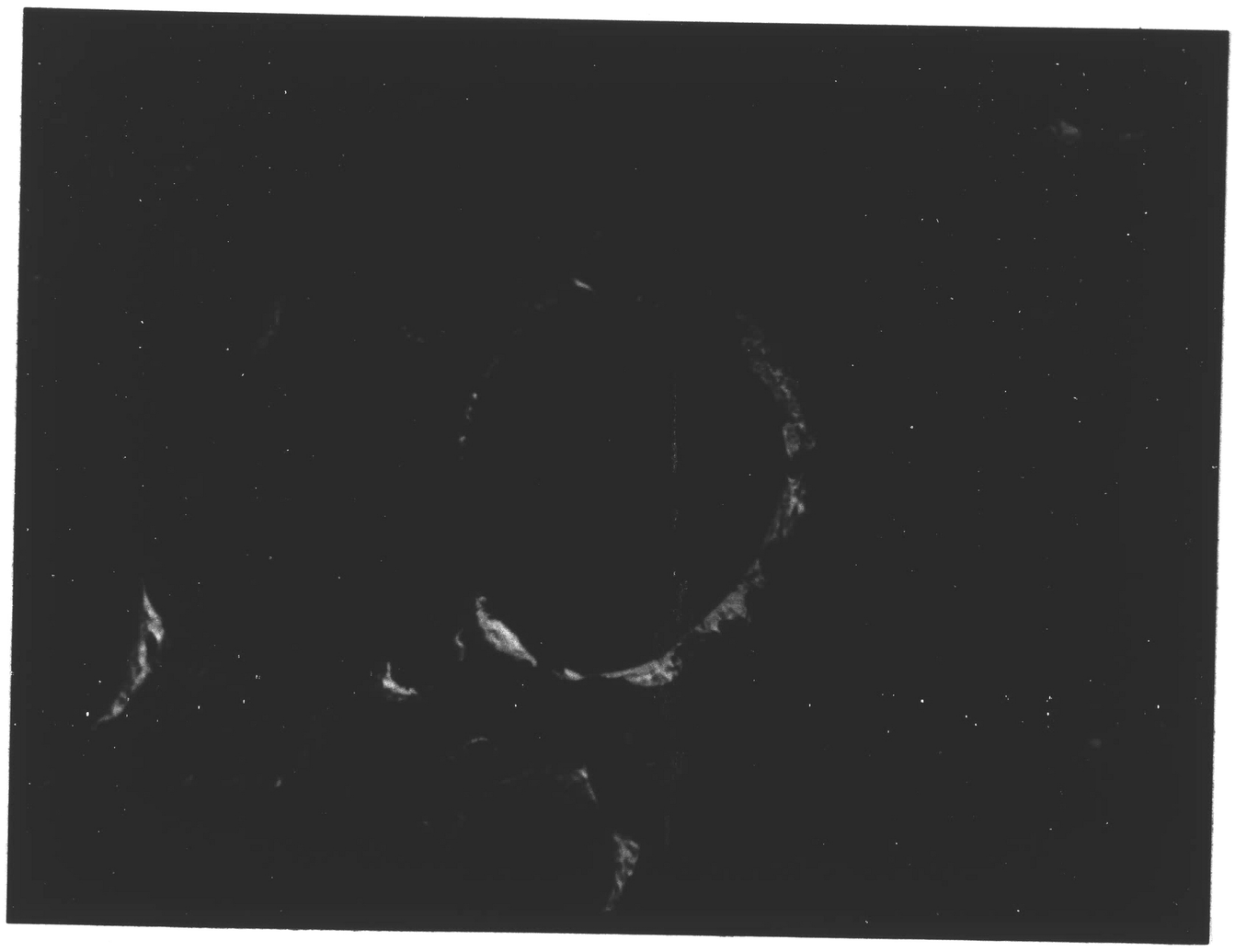

9A
500X

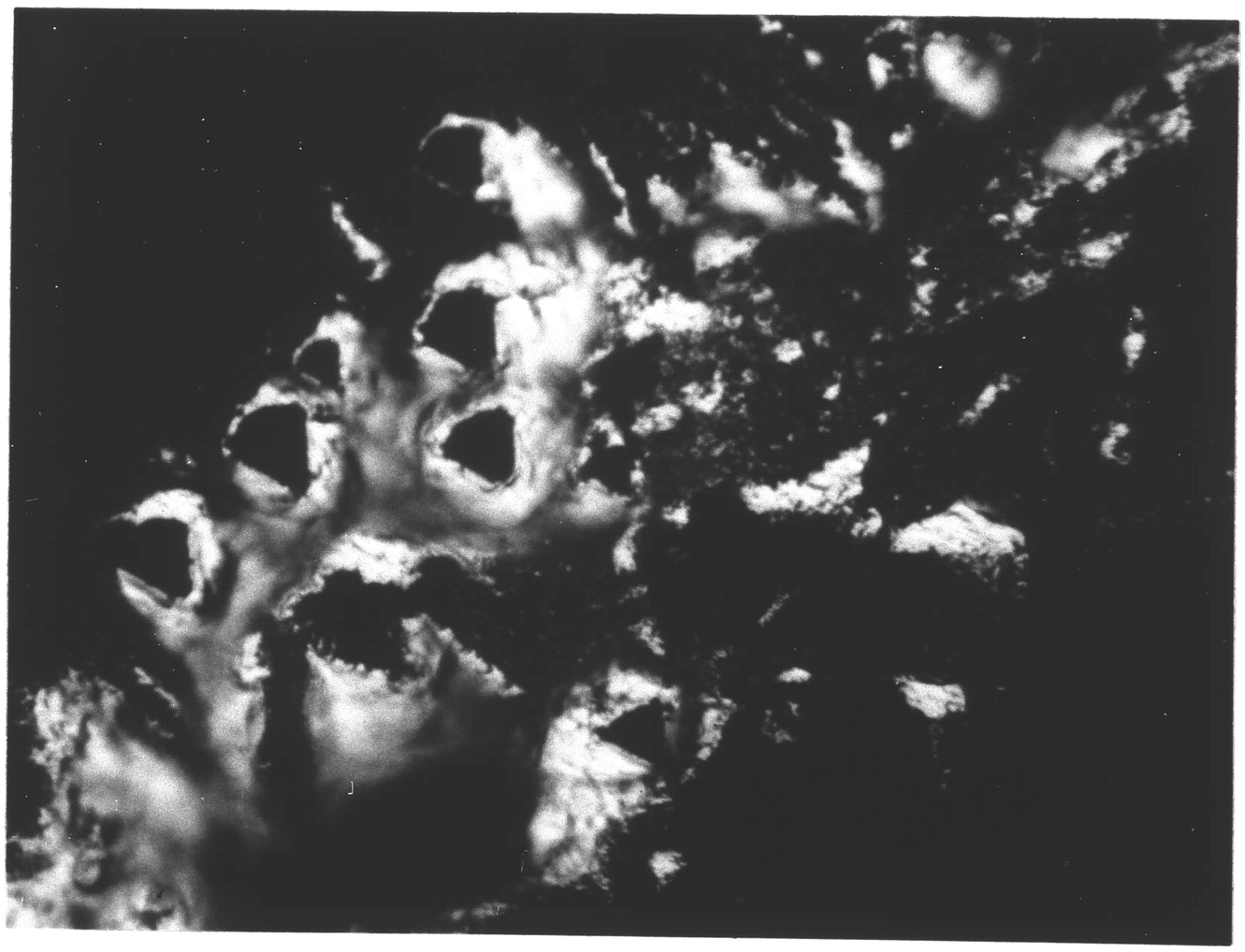

9B
500X

SAPPHIRE SURFACE AFTER TENSILE TEST

FIGURE 9

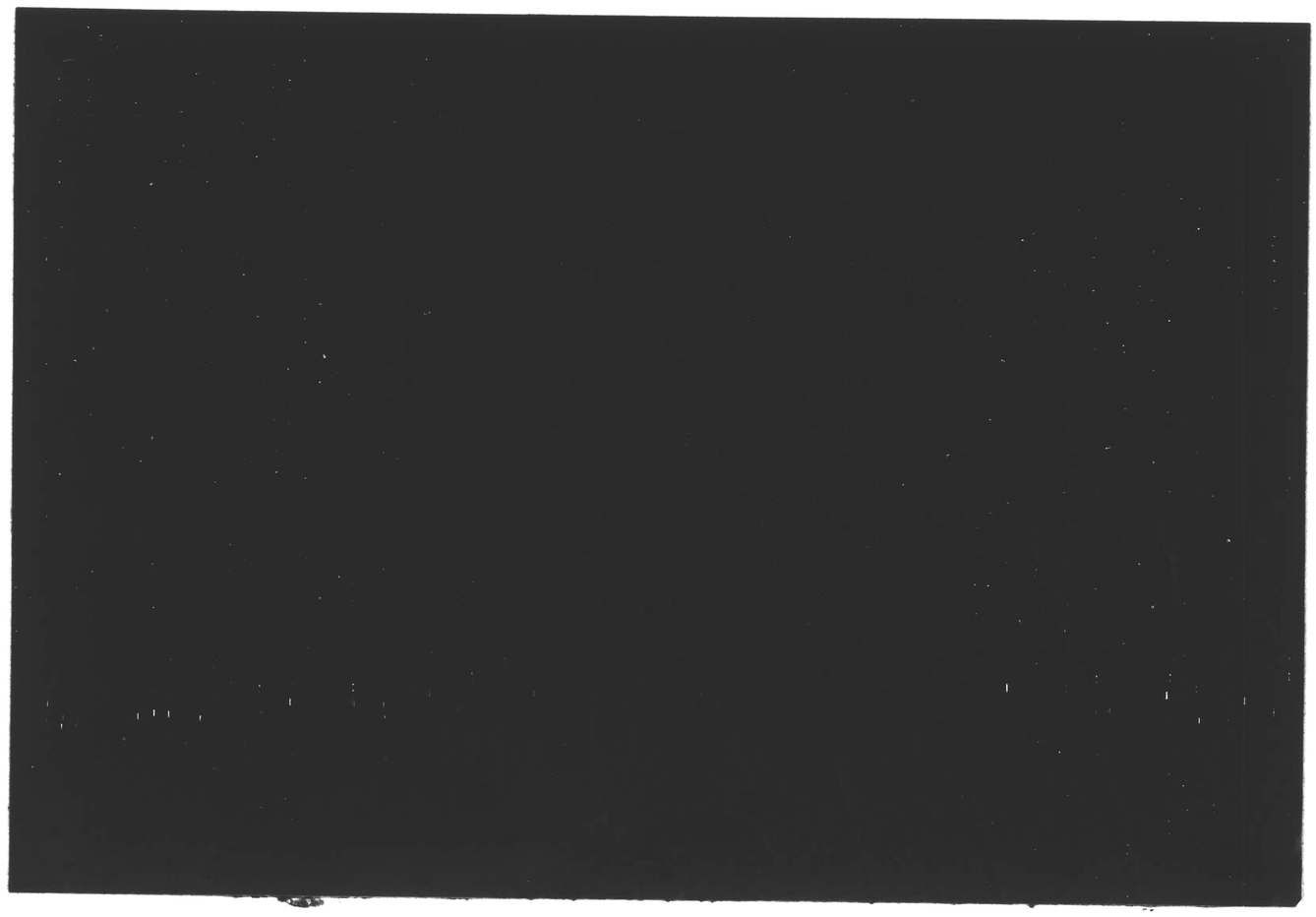

10A
200X

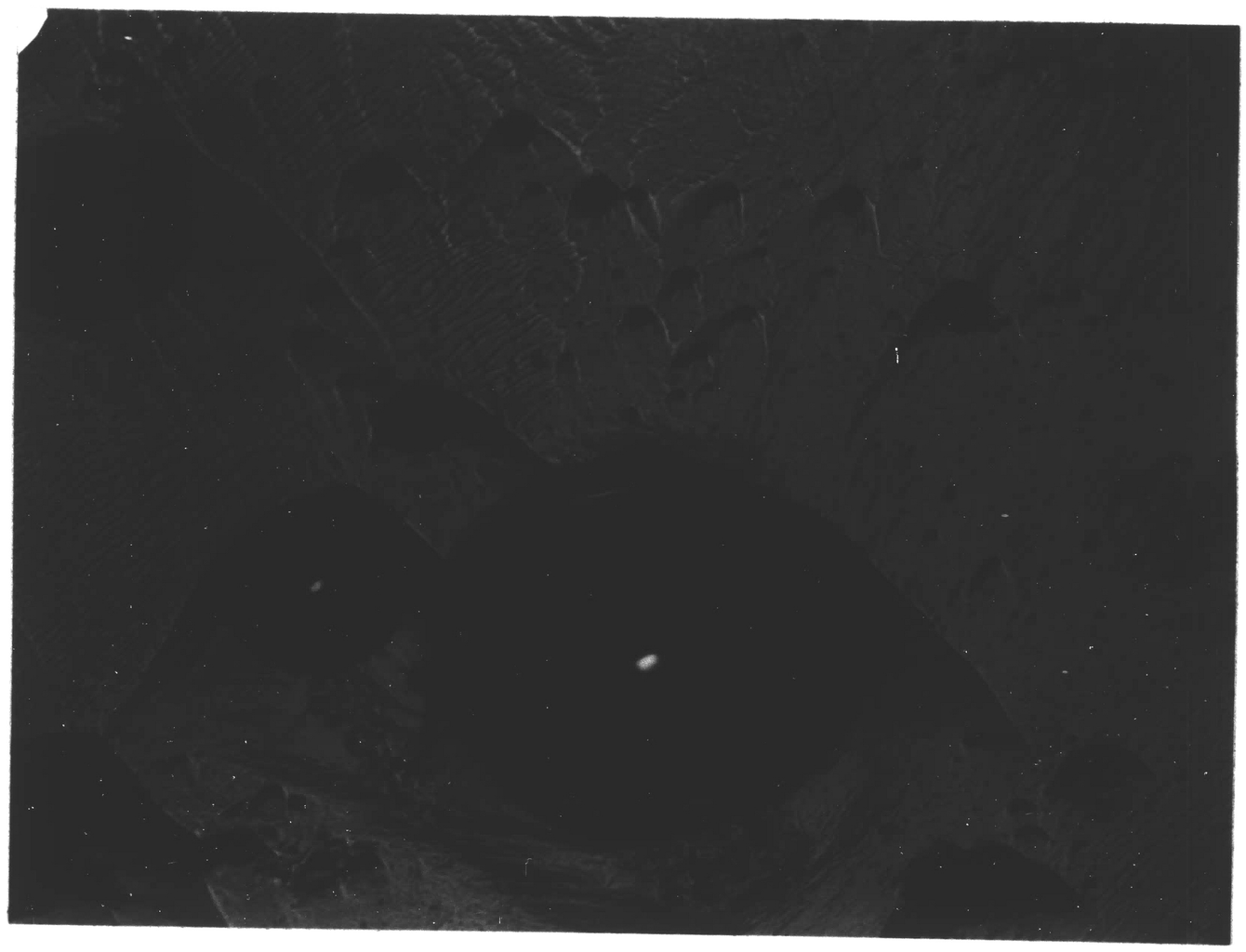

10B
100X

OXYGEN PROCESSED GOLD

FIGURE 10

The undesirable effects of interfacial gas occlusions is illustrated in Figure 10B. Many of the gas occlusions are flanked by ridges in the gold surface. This indicates that the occlusions enhance crack propagation.

V DISCUSSION

1. Effects of Oxygen Partial Pressure on Strength

One of the major goals of this thesis was to detect the partial pressure of oxygen needed to form strong adhesion couples. From the work of Moore and Thornton[14] it was estimated that the partial pressure of oxygen needed to produce oxide formation and good bonds would be approximately 50 torr. They report a peak in the adhesion of gold/glass couples at 150 torr oxygen pressure. Partial oxygen pressures in this range require low hydrogen: water vapor ratios, thus the hydrogen furnace work was limtied to the consideration of very low oxygen partial pressures only. Rossing[36] has also reported that nickel alloy adherence to alumina is dependent on oxygen partial pressure. It is reported that the oxygen pressure at which adherence maximized was dependent on alloy composition. The adherence increased with oxygen pressure until a critical degree of reaction at the interface occurred. Beyond this point the adherence decreased for increasing oxygen pressure. The inference is that an optimum interfacial layer of reaction products produces the strongest bonding.

The oxygen partial pressure data from the hydrogen samples and the data from the argon-oxygen gas mixtures is combined in Figure 11. It is seen that a strength increase of nearly an order of magnitude occurs between essentially zero oxygen pressure and 15 torr (2 percent oxygen). A peak in the adherence of the materials was not detected. The strength values obtained for pure argon processed

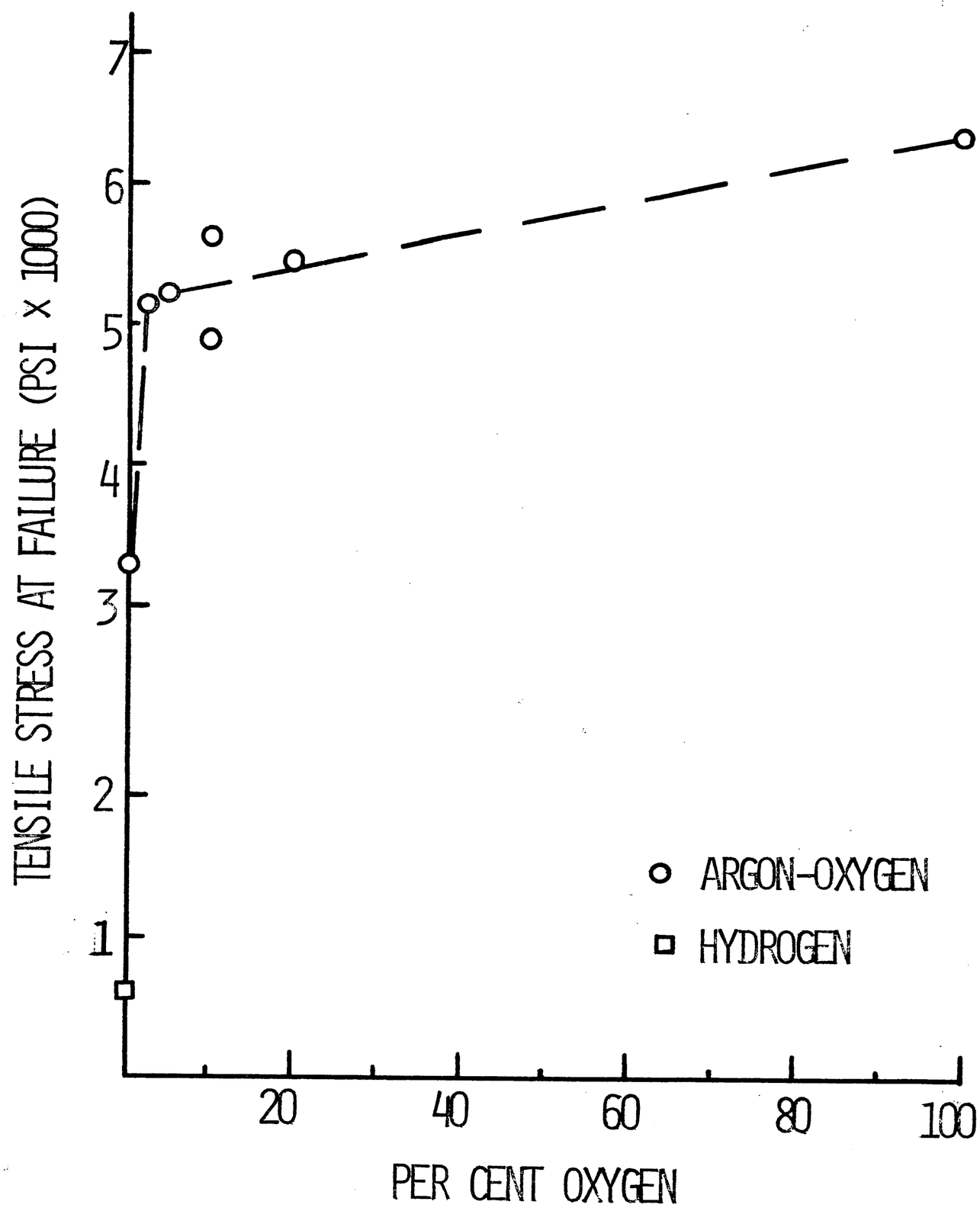

STRENGTH VS AMBIENT OXYGEN CONTENT

FIGURE 11

samples shows a surprising reproducibility in view of the fact that the curve is quite steep in this region. The samples heated to 500°C in oxygen followed by the normal argon cycle also have a similar strength. This indicates that oxygen must be present at the higher temperatures to form a strong adhesion couple. The observed strength for these samples could be caused by surface adsorbed oxygen which is not removed during the thermal cycle. This is suggested as a possible explanation for the uniform strength data obtained in these tests.

Moore and Thornton[14] report that the adhesion of gold/glass couples was concentrated at the perimeter of the drops. The enhanced strength at the perimeter was related to the diffusion of gold oxide into the glass. Radioactive gold tracers were used to verify that gold diffusion did occur. It was found that the gold tracer concentration was greatest at the drop perimeter. The surface tension forces cause a stress in this region which increases the diffusion rate. The bonding of the gold-sapphire system is not predominant at the perimeter as suggested above. This is shown in the photomicrographs obtained obtained from two samples which could not be tested to failure. The interface as viewed through the sapphire disc is shown in Figures 12A and 12B. It is seen that the gold has peeled away from the sapphire disc at the drop perimeter, but the adhesion couple has maintained sufficient strength to resist complete failure. There is no ring of gold marking the original perimeter position as reported previously[20]. Slight traces

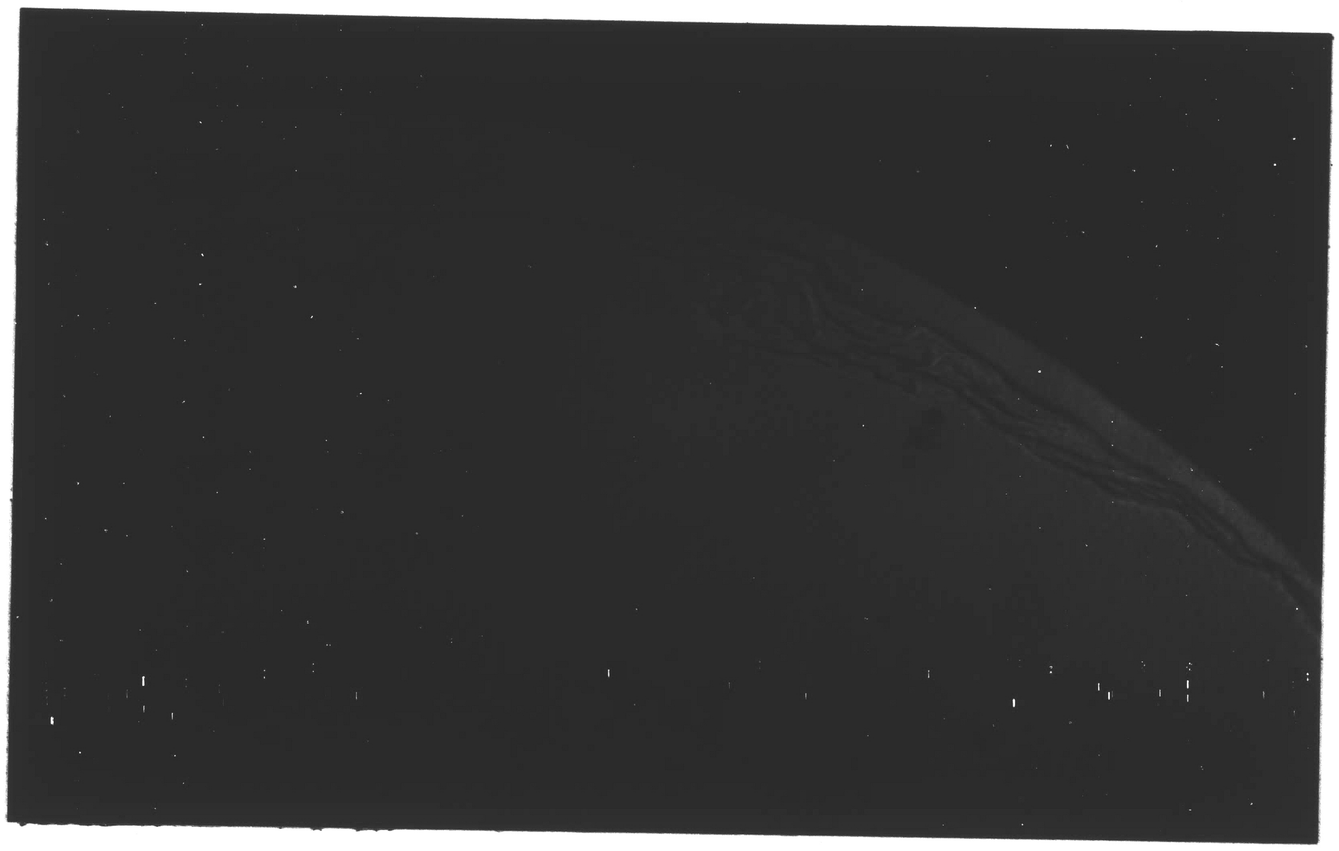

12A
100X

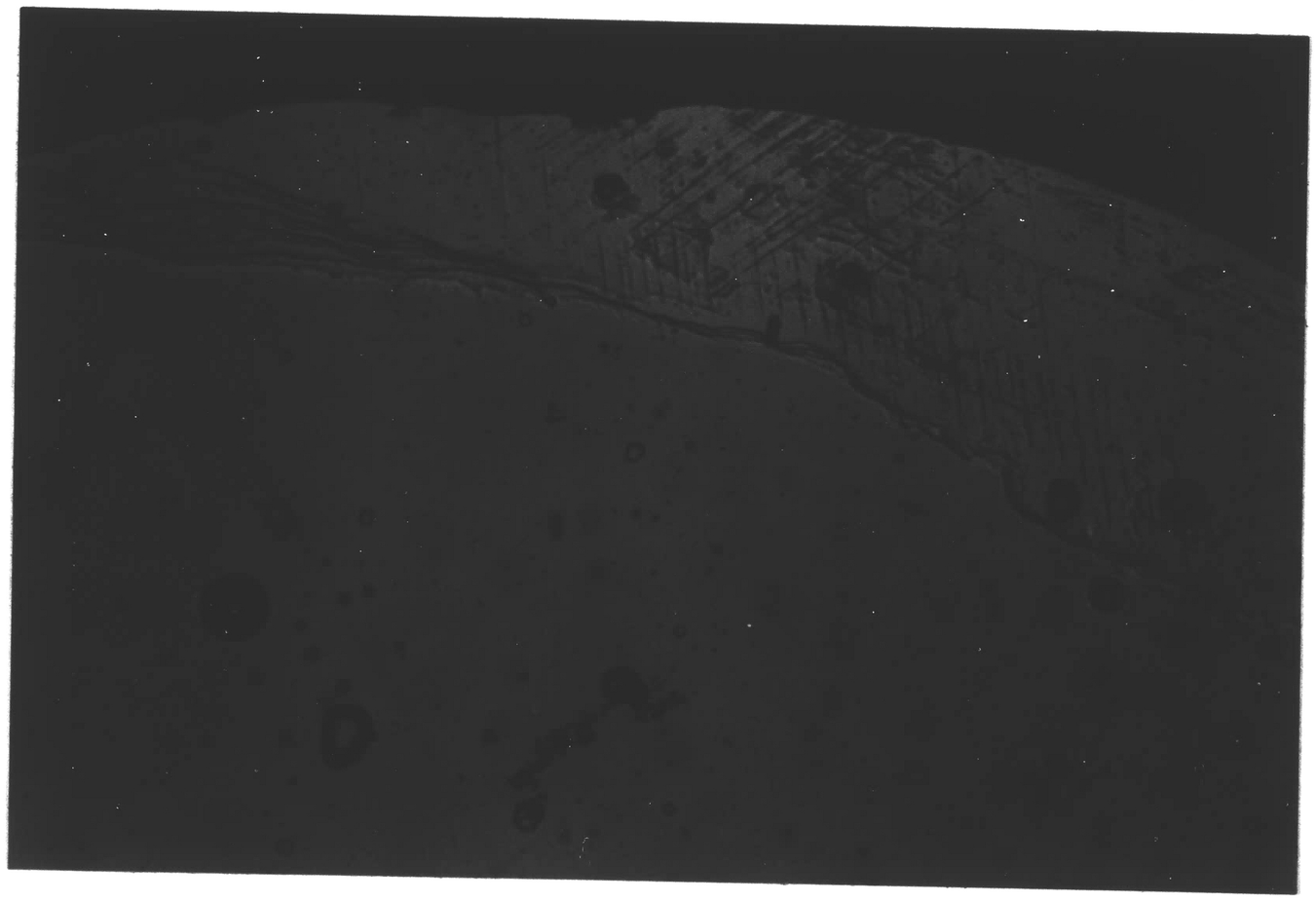

12B
100X

PARTIAL FAILURE OF ADHESION COUPLES

FIGURE 12

of gold marking the perimeter were found in only a few cases.

2. Oxide Diffusion Bonding Model

A model has been proposed[20] to describe the adhesion of gold to sapphire. The model assumes that when gold/sapphire adhesion couples are prepared in an oxygen atmosphere, an oxide of gold is formed. It is proposed that the gold oxide layer in the interface region diffuses into the sapphire at a rate dependent on the self diffusion rate of oxygen in sapphire. The surface tension forces at the interface perimeter are assumed to form a seal preventing the entrance of additional oxygen (gas phase) to the interface region. As the gold oxide layer (assumed to support no tensile stress) is depleted by diffusion into the sapphire, the "atomically clean" surfaces of gold and sapphire come to closer proximity. The adsorbed layer(s) of oxygen at the interface between the gold and sapphire are thus eliminated by the oxidation/diffusion process. The forces of attraction between the gold and sapphire are assumed to be primarily van der Waal dispersion forces.

Increases in the strength of the adhesion couple with time, for constant temperature processing, should be proportional to this oxidation/diffusion process. Since the self diffusion rate of oxygen in sapphire is not known at the temperature of interest a priori, it is necessary to proceed in reverse order to test the validity of the proposed model. That is, one can calculate to a reasonable approximation the maximum values of the dispersion forces. By using the maximum theoretical force, the general equation for the force, and

the separation distance of the gold/sapphire adhesion couple expressed as a function of time, it is possible to relate the observed strength to the oxygen self diffusion coefficient at a fixed temperature. This fixed temperature being the temperature used in preparing the adhesion couples. It is necessary to process the adhesion couples for various times at the same fixed temperature to establish that the tensile strength of the couples is dependent on the processing time. Equations have been developed to enable a comparison of the predicted diffusion coefficient based on the bonding model, to the measured[35] self diffusion coefficient. The equations will be presented later in this discussion.

The average stress and the maximum stress from Table 5 are plotted vs the square root of time in Figure 13. The data show a generally uniform increase in strength for increased time at temperature. The data also show a definite loss of average strength for the longest times used. The stress at failure values presented here are all generally greater than those reported previously[20], except for the longer times. This deviation from previous results is believed to be related to the method used in testing the samples.

The plot of Figure 13 establishes a time dependence relation for the observed stress at failure over a moderately broad time span (1 to 10 hours). Using the maximum stress values from Table 5 and the equations presented by Brandner[20] the values listed in Table 6 are calculated. The equations used for these computations are as follows:

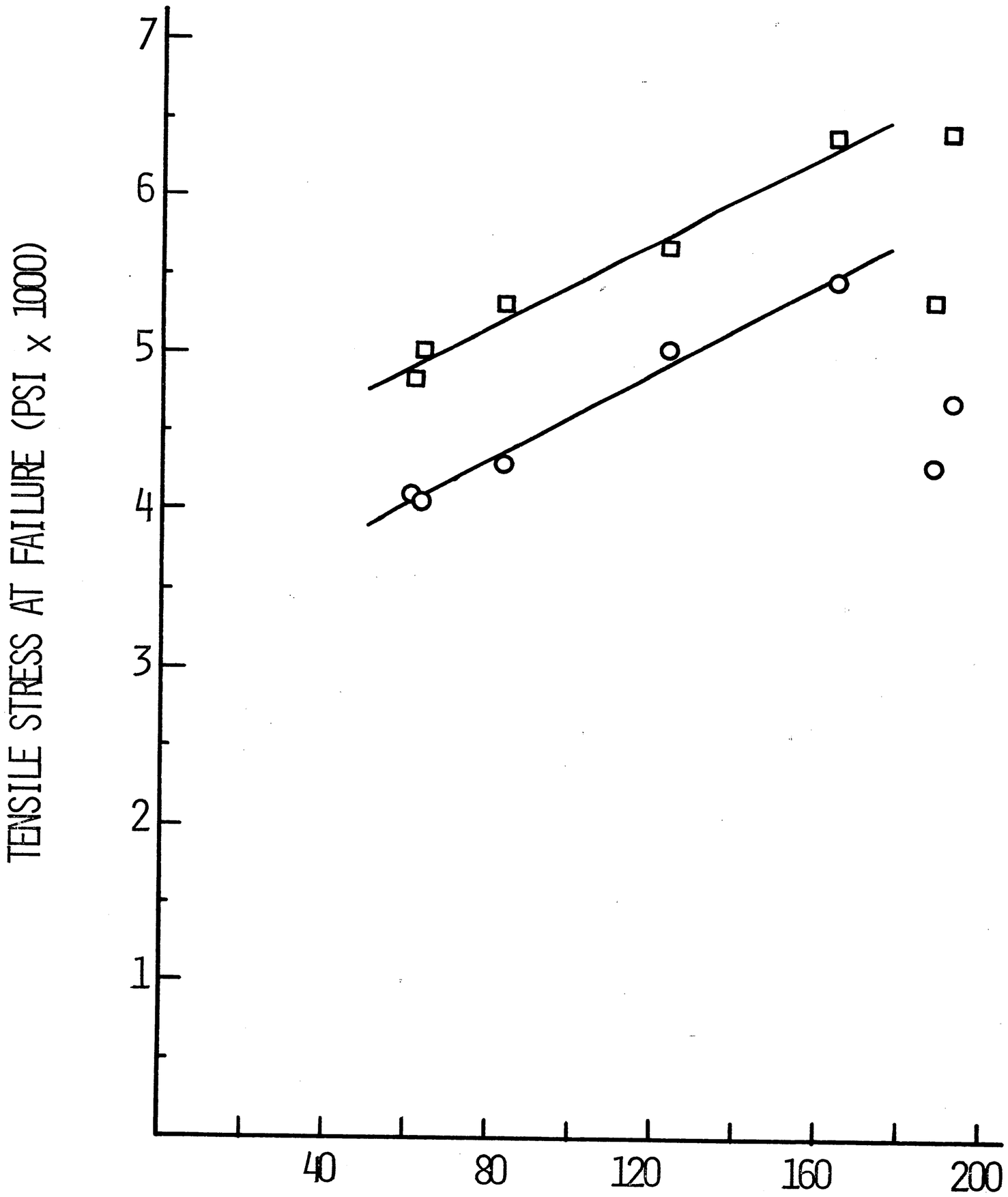

BOND STRENGTH VS TIME

FIGURE 13

TABLE 6

DATA FOR DETERMINING DIFFUSION COEFFICIENT

Run No.	Square Root of Time	S_m/S_o	d(t)
2	61.5	40.0	6.05
3	63.5	38.6	5.95
7	84.0	36.4	5.78
4	124.0	34.0	5.61
10	162.0	30.2	5.28

d(t) is calculated from equation (4)

(1) $$S_m = \frac{K}{r_m^3}$$

where S_m = the maximum theoretical van der Waal bond stress.

$= 1.33 \times 10^9$ dynes per square cm.

= 193,000 pounds per square inch.

K = the adhesion constant for the gold-sapphire system.

$= 2.08 \times 10^{-13}$ ergs

r_m = separation distance at maximum stress.

$= 2.5 \times 10^{-8}$ cm.

A review of the development of this equation for the gold-sapphire system revealed a minor error which has been corrected in the above values. This is discussed more completely in Appendix II. Equation (1) has the general form

(2) $$S_o = \frac{K}{d^3}$$

where S_o = the observed stress

d = the separation distance of the materials as tested.

From considering the diffusion of gold oxide into the sapphire at constant temperature and pressure, the separation of the materials as a function of time is

(3) $$d(t) = d_o - 2\left[\frac{Dt}{\pi}\right]^{1/2}$$

where $d(t)$ = time dependent separation distance.

d_o = the initial separation distance assumed constant for all samples.

D = oxygen self diffusion coefficient.

t = time

An additional relation for d(t) is obtained from considering the maximum stress and the observed stress

$$(4) \qquad d(t) = r_m \left[(S_m/S_o)^{1/3} - 1 \right]$$

where all terms have been defined.

From the inverse cube relation in equation (2) it may be expected that the observed stress vs square root of time plot would not be linear; however substituting (3) into (2) and expanding with a negative exponent

$$(5) \qquad S_o = Kd_o^{-3} + 3Kd_o^{-4} \left[\frac{Dt}{\pi} \right]^{1/2} - 6Kd_o^{-5} \left[\frac{Dt}{\pi} \right] + \ldots\ldots$$

it is seen that the higher order terms will drop out because D is a small number. In this case the expected value is less than 10^{-18}. The generally linear curve of Figure 4 is therefore an indication that the bonding mechanism involves a diffusion process. The model assumes that the oxidation/diffusion process acts to reduce the thickness of the gold oxide layer in the interface region.

It is interesting to note that the average stress for the argon processed couples listed in Table 2 corresponds well with the value

obtained by extrapolation of the average stress curve in Figure 13 to the point (t = 0). Argon is an inert gas and is not expected to react with nor to diffuse into the liquid gold drop. This being true, the argon data also tends to support a time dependent stress of the form given by equation (5). The argon strength would thus correspond to the first term on the right hand side of the equation.

The data of Table 6 are used in the plot of Figure 14. The curve is extrapolated to determine the initial separation. The slope of the curve is proportional to the diffusion coefficient as shown by equation (3). From the curve these values are

$$d_o = 6.4 \times 10^{-8} \text{ cm.}$$

$$D = 3.8 \times 10^{-21} \text{ cm}^2/\text{sec.}$$

The predicted initial separation distance corresponds to an average of slightly more than three monolayers of gas at the interface region. This is a readily acceptable value since the samples were made at an elevated temperature. It is known that adsorbed gases are removed at higher temperatures; however, removal of the innermost adsorbed layers normally requires a combination of high temperature and high vacuum. The net change in the separation distance is small in magnitude, though it corresponds to approximately 15 per cent of the original value.

The value of D as obtained from Figure 14 is shown in the plot of Figure 15. The straight line is based on an equation proposed by Oishi and Kingery[35] for the self diffusion coefficient of oxygen

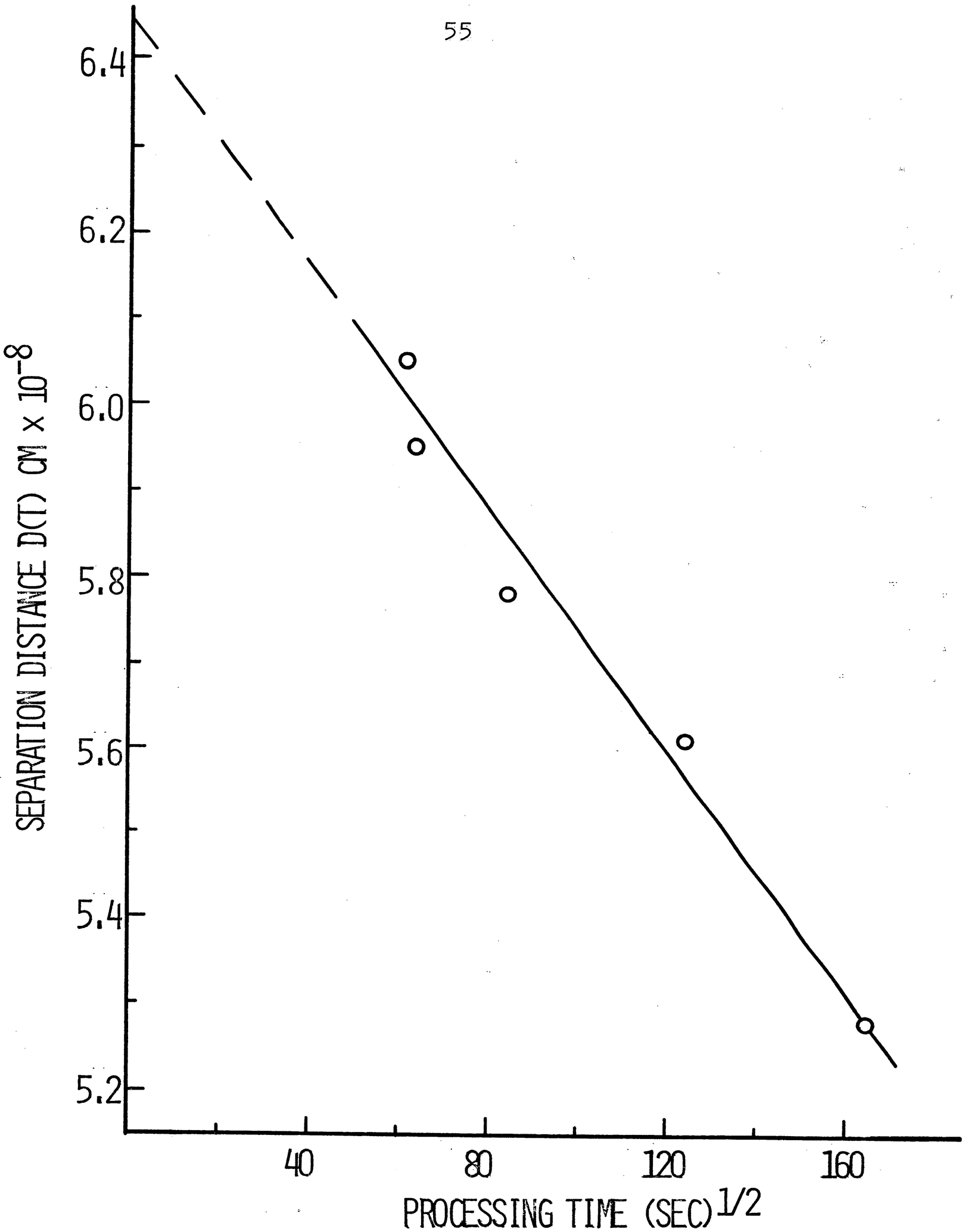

THEORETICAL SEPARATION OF MATERIALS

FIGURE 14

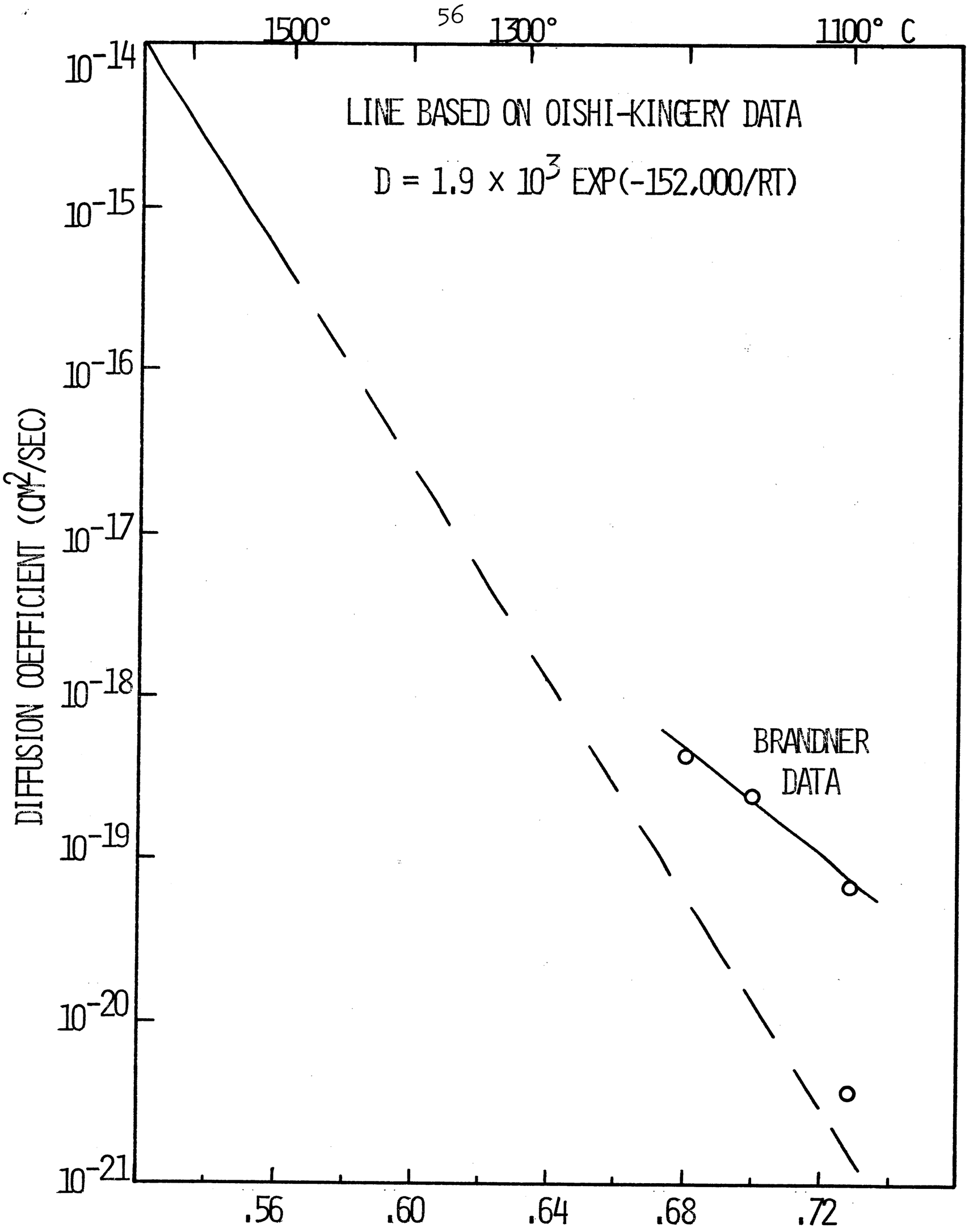

OXYGEN SELF DIFFUSION IN ALUMINA

FIGURE 15

in sapphire single crystal grains. A direct comparison is thus possible only by extrapolation over five orders of magnitude. It is seen that the value of D noted above lies very near the extrapolated line. The short line segment drawn through three points represents other published data[20]. The values shown at 1150° and 1200°C for this line are based on rather limited data, hence the reason for this attempt to expand upon the proposed model.

An effort was made to obtain data at a higher temperature. It was found that the bond strength did not increase as expected (see Run 12 data). The observed strengths at 1200°C were lower than those at 1100° for equal processing times. This problem is similar to the unexpected decrease in strength noted previously for samples held for long times at the lower temperature. Difficulties in obtaining meaningful and reproducible data at the higher temperatures were also reported previously[20]. This model has given an acceptable value for the initial separation distance, and a good estimate for the diffusion coefficient. The model fails, however, to explain the results obtained for long processing times, and also fails for higher temperatures. It is therefore proposed that there is another mechanism which is the predominant factor governing the adhesion of this system. An alternate adhesion mechanism is discussed in the following section.

3. Oxide Interlayer Bonding Model

It is proposed that the cause of the failure of the preceding model is related to the physical structure of the interface. During

microscopic examination of the adhesion couples it was noted that all samples have gas occlusions at the interface. Frequently the gas occlusions intersect as shown in Figure 16. The reduced strength, noted for longer processing times in oxygen, was accompanied by the appearance of extensive fields of negative crystals at the interface as shown in Figure 17. It is proposed that the presence of the intersecting gas occlusions and negative crystals in the interface are caused by the precipitation of dissolved gas in the liquid metal during the cooling process. Such segregation or precipitation of solute at grain boundaries, interfaces, or other structural discontinuities is commonly observed. If the gas occlusions had been in contact during the time the gold was molten, the surface tension forces would have caused the bubbles to coalesce quickly. In the photomicrographs in Figure 16 it is seen that the points of intersection are distinct. An additional reflection from the wall initially separating the occlusions is also clearly visible. There is no reason to suspect that some of the smaller occlusions would have been polyhedral shapes while the gold was molten, but that they could have grown to form polyhedral shapes as shown by the form of the negative crystals seems reasonable. From the extent of the negative crystal structures in the interface shown in Figure 17 it appears that some of these shapes must have been nucleated by gas precipitation during the cooling cycle. The work done with various other gas environments tends to confirm the above analysis of the interfacial structure. Shrinkage of the metal during cooling

16A
100X

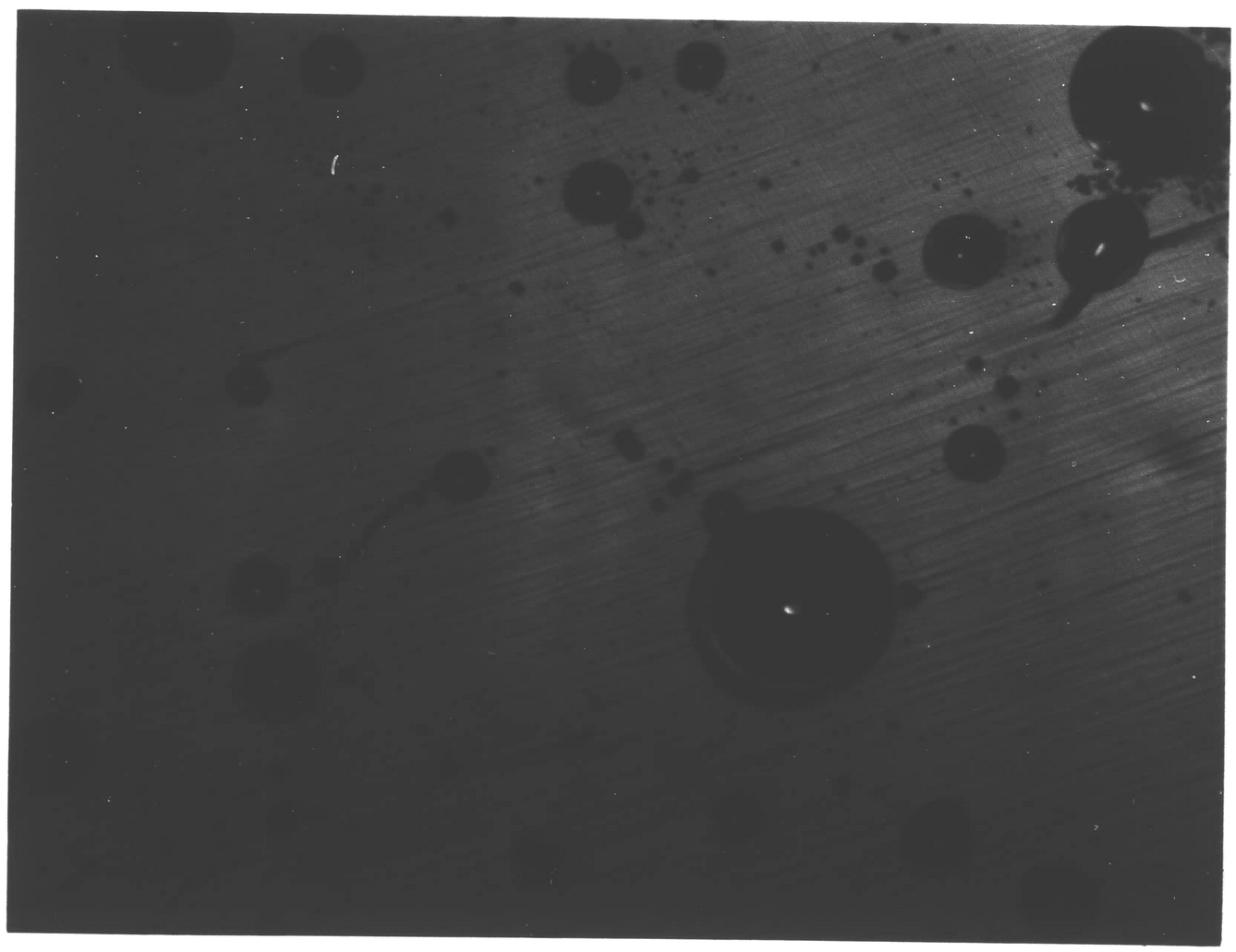

16B
100X

INTERSECTING GAS OCCLUSIONS

FIGURE 16

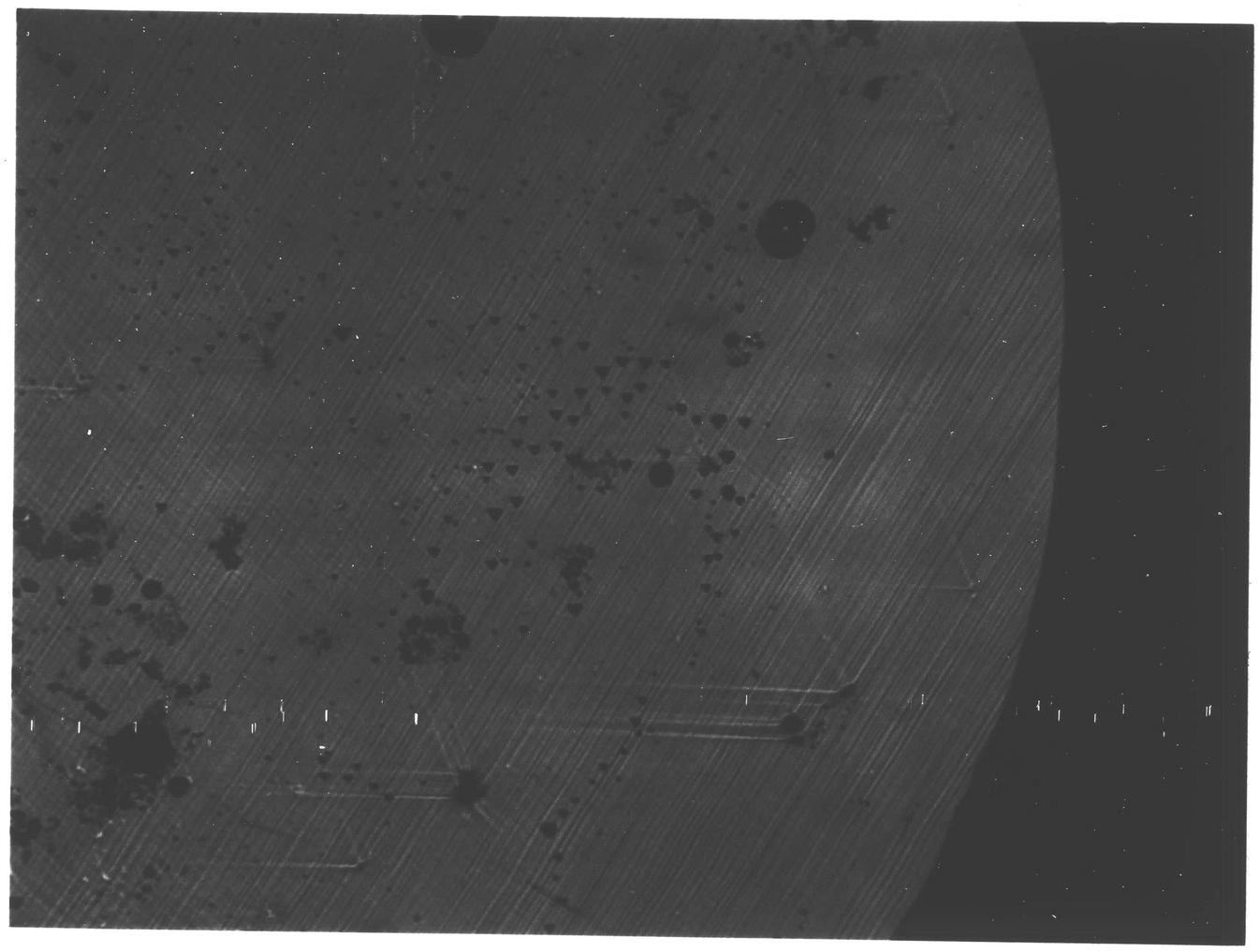

17A
100X

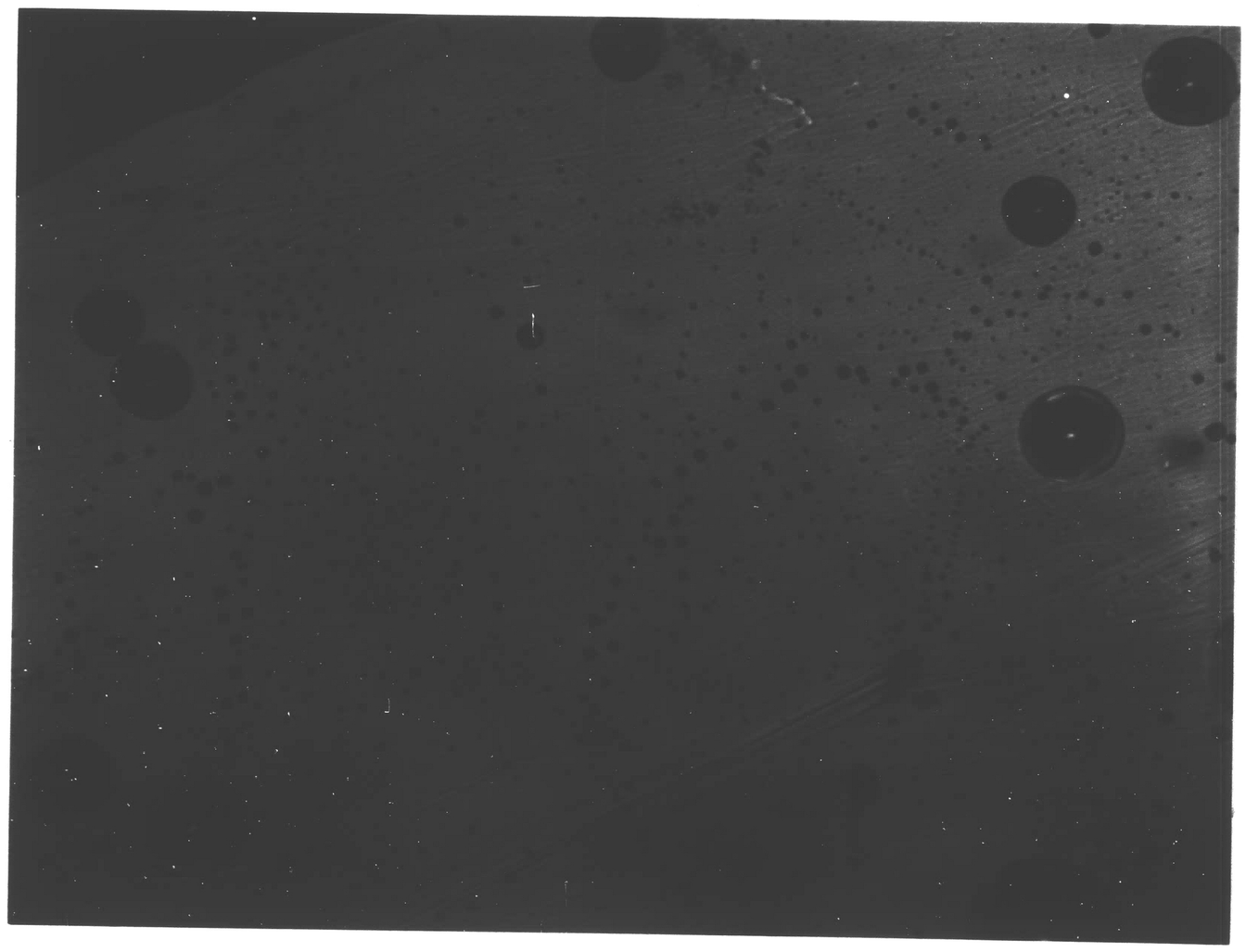

17B
100X

EFFECTS OF LONG TIME PROCESSING IN OXYGEN

FIGURE 17

could also cause void formations; however, this mechanism would not explain why the number of defects increased in those samples held at high temperature for longer times.

Therefore it is proposed that the adhesion of gold/sapphire adhesion couples is dependent on the formation of an oxide transition layer at the interface. It is suggested that the adsorbed layer of gas in the interface region diffuses into the liquid gold drop. The trapped gas in the interfacial occlusions is similarly dispersed. It is proposed that the adhesion increases with increased oxide layer thickness until a critical point is reached, beyond which the adhesion decreases.

The literature contains conflicting reports as to the existence of gold oxide at high temperature. Clark et al.[37] report that gold oxide is not formed after heating in oxygen at low pressure or in air at normal pressure. Shishakov[38] has criticized the report and indicates the existence of a surface peroxide. It is stated that the structure is hexagonal and contains oxygen molecules aligned parallel to the c axis. Reference is made to his book[39] which sites other examples of changes in the electron diffraction diagrams caused by heating gold in oxygen. Clark and associates issued a rebuttal[40] to this criticism indicating the correctness of their report.

The above discussion of gold oxide formation does not consider the effects of an adjacent surface. Since adhesion is a measure of the mutual attraction of adjacent surfaces, the interaction effects should be considered. An example of the effects of an adjacent

surface has been presented for nickel oxide[41]. Nickel forms one stable oxide in bulk form NiO, but substantial amounts of Ni_2O_3 have been grown on alumina surfaces. Similarly NiO_2 is the form which initially appears on titania surfaces. It is proposed that an interaction of this type results in the formation of the gold oxide transition layer. If the amount of oxygen in solution in the gold drop is too great, precipitation at the interface can occur. Oxygen is reported as being slightly soluble in liquid gold[41].

The effects of an adjacent surface on the possible formation of a surface gold oxide are also shown by Meyer[42]. In his work thin films of gold on bismuth oxide were studied. It is reported that by annealing the films at 350°C in air or oxygen, at normal pressure, a surface complex is formed. The detection of the complex is related to conductivity changes and to the mechanical behavior of additional gold deposits on the annealed films. It is stated that overlayers of gold, vapor deposited, on the annealed films can be stripped away with scotch tape. The annealed film remains intact, indicating that some structural difference between the annealed film and the overlayer exists resulting in poor mutual adherence. The paper also lists other reports indicating the formation of gold oxide by heating gold in air or oxygen.

This bonding model is proposed primarily as an attempt to explain the observed physical structure of the interface region and its relation to the mechanical strength of the adhesion couples. Weyl[43] has previously suggested that an intermediate oxide layer could in-

crease the adhesion of metal/oxide pairs. Other reports[11,14,15,24] also indicate that improved adhesion results from an oxide interlayer.

VI CONCLUSION

From the tensile strength data presented previously it is clear that oxygen has a significant effect on the adhesion of the gold-sapphire system. The adhesion developed during oxygen processing exceeds the strength of gold in some areas as evidenced by the gold remaining on the sapphire surface after tensile testing. This study has also shown that minor amounts of oxygen in the ambient atmosphere are sufficient to produce good adhesion. The tensile stress at failure in this system increased by an order of magnitude from conditions of essentially zero oxygen partial pressure to an oxygen pressure of 15 torr.

A review of Brandner's oxide diffusion model has shown that van der Waal bonding is sufficient to account for the observed tensile strength for this system. The model yields good predictions in some cases, but fails to describe all of the observed adhesion characteristics. An alternate bonding mechanism has been proposed, which is based on the observed structure of the adhesion couple interfacial area. This mechanism accounts for the observed peak in adhesion noted in those samples held at high temperature for longer times.

The tensile testing apparatus developed during this study has given good reproducible results and could be used for other systems where the contact angle is sufficiently great to allow firm gripping of the sessile drop. The strength changes noted for minor modifications are again a reflection of the difficulties inherent to obtaining a truly representative measure of adhesion.

APPENDIX I

Experimental Data

Data values marked with an asterisk are samples which could not be tested to failure. The tabulated data are listed as area in square inches, load in pounds, and stress in pounds per square inch.

Run No. 1 Gold-Oxygen, 1100° C, 1:04 hrs.

Sample No.	Area	Load	Stress
1	0.00703	16.0	2276
2	0.00785	24.6	3134
3	0.00696	23.6	3391
4	0.00596	21.3	3574
5	0.00739	23.5	3180
6	0.00801	17.6	2197
7	0.00749	22.0	2937
8	0.00701	24.8	3538
9	0.00676	27.6	4083

Average Stress = 3145 psi

Contact Angle = 127°

Warm Air Stream Drying

Run No. 2 Gold-Oxygen, 1100° C, 1:03 hrs.

Sample No.	Area	Load	Stress
1	0.00920	37.8	4109
2	0.00930	38.9	4183
3	0.00911	38.8	3710
4	0.00979	37.5	3830
5	0.00964	46.5	4824
7	0.00969	37.0	3818
8	0.00973	39.3	4039
9	0.01032	42.5	4118

Average stress = 4079 psi

Contact angel = 116°

Run No. 3 Gold-Oxygen, 1100° C, 1:07 hrs.

Sample No.	Area	Load	Stress
1	0.00950	37.6	3958
2	0.00954	34.0	3564
3	0.00989	34.5	3488
4	0.00998	48.4	4850
6	0.00986	29.8	3022
7	0.00978	37.8	3865
8	0.01001	50.1	5005
9	0.00907	41.9	4620

Average stress = 4046 psi

Contact angel = 116°

Run No. 4 Gold-Oxygen, 1100° C, 4:16 hrs.

Sample No.	Area	Load	Stress
1	0.00895	40.0	4469
2	0.00837	43.1	5149
3	0.00830	42.8	5156
4	0.00924	42.4	4588
5	0.00923	51.0	5525
6	0.00870	49.3	5666
7	0.00773	29.0	3751
8	0.00866	48.3	5577
9	0.00954	50.5	5293

Average stress = 5019 psi

Contact angle = 114°

Run No. 5 Gold-Oxygen, 1100° C, 10:15 hrs.

Sample No.	Area	Load	Stress
1	0.00933	46.0	4930
2	0.00941	60.3	6408
3	0.00945	43.3	4582
4	0.00920	31.0	3370
5	0.00911	36.0	3952
6	0.00930	43.8	4710
7	0.00949	37.9	3994
8	0.00899	44.3	4928
9	0.00934	49.6	5310

Average stress = 4687 psi

Contact angle = 112°

Run No. 6 Gold-Oxygen, 1100° C, 9:52 hrs.

Sample No.	Area	Load	Stress
1	0.00955	24.0	2513
2	0.00918	47.2	5142
3	0.00960	30.8	3208
4	0.00978	43.5	4448
5	0.00915	48.5	5300
6	0.00948	45.5	4800
7	0.00955	28.5	2984
8	0.00938	44.5	4744
9	0.00937	50.0	5336

Average stress = 4275 psi

Contact angel = 113°

Run No. 7 Gold-Oxygen, 1100° C, 1:58 hrs.

Sample No.	Area	Load	Stress
1	0.0153	49.0	3202
2	0.0148	78.5	5304
3	0.0152	69.3	4559
4	0.0152	67.4	4434
5	0.0152	58.8	3868
6	0.0151	67.4	4464
7	0.0151	55.1	3649
8	0.0153	62.2	4065
9	0.0154	78.0	5065

Average stress = 4290 psi

Contact angle = 113°

Run No. 8 Gold-Argon, 1100° C, 1:02 hrs.

Sample No.	Area	Load	Stress
1	0.01077	17.2	1597
2	0.01155	42.6	3688
3	0.01358	50.0	3682
4	0.01302	60.1	4616
5	0.01124	27.3	2429
6	0.01277	50.2	3931
7	0.01263	30.0	2375
8	0.01288	51.1	3967

Average stress = 3286 psi

Contact angle = 124°

Run No. 9 Gold-Argon, 1100° C, 1:08 hrs.

Sample No.	Area	Load	Stress
1	0.01459	52.0	3564
2	0.01413	35.6	2519
3	0.01280	47.3	3695
4	0.01352	42.0	3106
5	0.01455	46.7	3210
6	0.01437	65.0	4523
7	0.01457	68.1	4674
8	0.01311	19.4	1480
9	0.01451	49.3	3398

Average stress = 3352 psi

Contact angle = 120°

Run No. 10 Gold-Oxygen, 1100° C, 7:15 hrs.

Sample No.	Area	Load	Stress
1	0.01571	94.0	5983*
2	0.01552	92.0	5928
3	0.01555	61.8	3974
4	0.01570	82.6	5261
5	0.01576	79.1	5019
6	0.01611	103.0	6394*
7	0.01533	91.8	5911*
8	0.01531	87.9	5741
9	0.01541	77.2	5010

Average stress = 5469 psi

Contact angle = 112°

Run No. 11 Gold-Argon, 1100° C, 1:00 hrs.

Sample No.	Area	Load	Stress
1	0.01382	47.2	3415
2	0.01393	52.0	3733
3	0.01174	28.4	2419
4	0.01388	47.8	3444
5	0.01322	41.8	3162
6	0.01616	68.0	4208
7	0.01362	47.5	3487
8	0.01436	53.5	3726
9	0.01235	42.2	3417

Average stress = 3445

Contact angle = 118°

Run No. 12 Gold-Oxygen, 1200° C, 1:00 hrs.

Sample No.	Area	Load	Stress
1	0.00968	38.6	3988
2	0.00994	38.9	3914
3	0.00892	33.7	3778
4	0.00953	38.3	4019
5	0.00984	40.8	4146
6	0.00984	40.3	4096
7	0.00987	32.4	3283
8	0.01006	34.4	3419
9	0.00949	30.7	3235

Average stress = 3764 psi

Contact angle = 116°

Run No. 13 Gold-Vacuum, 1100° C, 1:00 hrs.

Sample No.	Area	Load	Stress
1	0.01241	87.8	7075*
2	0.01330	103.0	7744*
3	0.01331	98.5	7400*
4	0.01267	93.1	7348
5	0.01311	101.0	7704*
6	0.01270	106.0	8346*
7	0.01332	101.5	7620*
8	0.01485	98.2	6613
9	0.01311	104.0	7933*
Retested with Modified Grip			
2	0.01330	132.0	9920*
3	0.01331	120.0	9016**

Contact Angle = 118°

Note: The double asterisk indicates that the disc broke in half.

Run No. 14 Gold-Hydrogen, 1100° C, 0:55 hrs.

Sample No.	Area	Load	Stress
10	0.00868	Broke putting on grip	
11	0.00788	Same as above	
12	0.00836	1.8	215
13	0.00832	6.7	814
14	0.00831	5.3	638
16	0.00842	7.9	938
17	0.00836	1.4	167
19	0.00792	5.1	644

Average stress = 569 psi

Contact angle = 121°

Run No. 15 Gold-Hydrogen, 1100° C and cool

Sample No.	Area	Load	Stress
10	0.00841	5.4	642
11	0.00825	Broke putting on grip	
12	0.00853	5.2	610
13	0.00797	4.8	602
14	0.00838	2.3	274
16	0.00821	9.2	1120
17	0.00844	4.0	474
18	0.00814	3.6	442
19	0.00732	1.7	232
20	0.00791	3.5	443

Average stress = 538 psi

Contact angle = 123°

Run No. 16 Gold-Air, 1100° C, 1:45 hrs.

Sample No.	Area	Load	Stress
10	0.00927	49.2	5307
11	0.00897	42.1	4693
12	0.01025	79.4	7746
13	0.00996	62.2	6245
14	0.00930	45.3	4871
16	0.00946	52.4	5539
17	0.00965	38.1	3948
18	0.00969	57.0	5882
19	0.00944	40.8	4322
20	0.00997	84.3	8455*

Average stress = 5700 psi

Contact angle = 116°

Run No. 17 Gold-Nitrogen, 1100° C, 1:18 hrs.

Sample No.	Area	Load	Stress
10	0.00858	23.5	2739
11	0.00839	29.7	3540
12	0.00859	44.5	5180
13	0.00897	15.5	1728
14	0.00807	39.0	4833
16	0.00847	32.5	3837
17	0.00845	36.5	4319
18	0.00898	29.5	3285
19	0.00836	29.0	3469
20	0.00886	27.0	3047

Average stress = 3598 psi

Contact angle = 120°

Run No. 18 Gold-Oxygen, 1100° C, 1:06 hrs.

Sample No.	Area	Load	Stress
10	0.01078	62.7	5816
11	0.01067	59.4	5567
12	0.00949	62.4	6575
13	0.01075	54.3	5051
14	0.00988	102.0	10220*
16	0.01055	40.2	3810
17	0.00986	79.9	8103
18	0.00870	47.0	5402
19	0.01081	91.3	8446
20	0.00993	53.5	5388

Average stress = 6439 psi

Contact angle = 116°

Run No. 19 Gold-Argon, 1100° C, 1:23 hrs.

Sample No.	Area	Load	Stress
10	0.00965	38.2	3958
11	0.00968	25.2	2603
12	0.00977	41.1	4207
13	0.00986	16.0	1623
14	0.00977	26.3	2692
16	0.00952	40.4	4244
17	0.00983	16.3	1658
18	0.00907	21.2	2337
19	0.01005	34.3	3413
20	0.00967	31.8	3288

Average stress = 3002 psi

Contact angle = 117°

Run No. 20 Gold-Argon, 1100° C, 1:00 hrs.

Sample No.	Area	Load	Stress
11	0.00905	12.9	1425
12	0.00957	28.8	3009
13	0.00979	39.4	4024
14	0.00896	16.2	1808
16	0.00868	28.7	3306
17	0.00915	17.8	1945
18	0.00879	24.0	2730
19	0.00997	28.4	2848
20	0.00937	16.7	1782

Average stress = 2542 psi

Contact angle = 118°

Run No. 21 Gold-Oxygen, 500° C, 0:15 hrs.

Gold-Argon, 1100° C, 1:08 hrs.

Sample No.	Area	Load	Stress
10	0.00900	34.3	3811
11	0.00901	39.0	4328
12	0.00960	29.5	3073
13	0.00927	39.6	4272
14	0.00886	34.9	3939
16	0.00932	16.4	1760
17	0.00907	27.3	3010
18	0.00920	31.2	3391
19	0.00949	30.8	3246
20	0.00920	20.5	2228

Average stress = 3306 psi

Contact angle = 118°

Run No. 22 Gold-10% Oxygen 90% Argon, 1100° C, 1:00 hrs.

Sample No.	Area	Load	Stress
10	0.00969	64.6	6667
11	0.00881	59.3	6731
12	0.00946	50.4	5328
13	0.00928	43.3	4666
14	0.00953	37.4	3924
16	0.00939	46.8	4984
17	0.00948	39.6	4177
18	0.00934	40.8	4368
19	0.00933	33.7	3612
20	0.00944	40.5	4290

Average stress = 4875 psi

Contact angle = 118°

Run No. 23 Gold-20% Oxygen 80% Argon, 1100° C, 1:04 hrs.

Sample No.	Area	Load	Stress
2	0.00885	48.3	5458
4	0.00952	41.3	4338
5	0.00929	57.2	6157
6	0.00941	53.3	5664
7	0.00938	51.4	5480
8	0.00927	53.2	5739
9	0.00924	52.8	5714

Average stress = 5507 psi

Contact angle = 118°

Run No. 24 Gold-Air, 1100° C, 1:00 hrs.

Sample No.	Area	Load	Stress
1	0.00991	40.7	4107
2	0.00938	63.6	6780
4	0.00924	41.0	4437
5	0.00969	54.2	5593
6	0.00916	57.1	6234
7	0.00999	47.8	4785
8	0.01089	55.1	5060
9	0.01032	58.4	5659
10	0.00941	36.5	3879
11	0.00985	66.1	6711
12	0.00949	34.2	3604
13	0.01060	47.0	4434
14	0.00967	46.3	4788
16	0.00898	47.3	5267
17	0.00945	54.8	5799
18	0.00950	60.0	6319
19	0.01046	43.1	4120
20	0.00948	54.2	5717

Average stress = 5185 psi

Contact angle = 118°

Run No. 25 Gold-50% Oxygen 50% Nitrogen, 1100° C, 1:06 hrs.

Sample No.	Area	Load	Stress
1	0.00776	43.0	5541
2	0.00709	46.8	6601
4	0.00733	37.3	5089
5	0.00702	37.6	5356
6	0.00741	40.0	5398
7	0.00760	48.0	6316
8	0.00718	45.8	6379
9	0.00819	40.9	4994
10	0.00770	33.6	4364
11	0.00806	35.9	4454
12	0.00819	41.4	5055
13	0.00744	28.7	3858
14	0.00827	43.6	5272
16	0.00751	40.3	5366
17	0.00693	34.3	4949
18	0.00772	45.2	5855
19	0.00765	41.6	5438
20	0.00864	39.9	4618

Average stress = 5272 psi

Contact angle = 128°

Run No. 26 Gold-5% Oxygen 95% Argon, 1100° C, 1:05 hrs.

Sample No.	Area	Load	Stress
1	0.00926	51.3	5540
4	0.00988	58.2	5891
5	0.00930	42.9	4613
6	0.00886	33.8	3815
7	0.00930	51.8	5570
8	0.00906	50.9	5618
9	0.00936	49.9	5331
10	0.00909	55.0	6051
11	0.00967	43.3	4478
12	0.00935	63.0	6738
13	0.00955	28.2	2953
14	0.00949	56.2	5922
17	0.00937	52.1	5560
18	0.00924	45.2	4891
19	0.00988	56.2	5688
20	0.01001	49.3	4925

Average stress = 5224 psi

Contact angle = 118°

Run No. 27 Gold-10% Oxygen 90% Argon, 1100° C, 1:08 hrs.

Sample No.	Area	Load	Stress
1	0.00924	26.8	2857
4	0.01008	67.1	6657
5	0.00950	70.8	7453
6	0.00928	37.7	4062
7	0.00950	62.4	6568
8	0.00998	73.2	7335
9	0.00980	48.9	4990
10	0.00926	62.5	6749
11	0.00971	55.3	5695
12	0.01015	61.7	6079
13	0.00947	52.6	5554
14	0.00925	49.4	5341
17	0.00985	44.1	4477
18	0.00954	53.9	5650
19	0.00952	54.9	5767
20	0.00953	42.4	4499

Average stress = 5605 psi

Contact angle = 118°

Run No. 28 Gold-2% Oxygen 98% Argon, 1100° C, 1:05 hrs.

Sample No.	Area	Load	Stress
1	0.00968	36.4	3760
4	0.00969	40.9	4221
5	0.00814	52.6	6462
6	0.01007	63.3	6286
7	0.00977	38.8	3971
8	0.00921	45.1	4897
9	0.00942	46.9	4979
10	0.00978	49.3	5041
11	0.00952	48.2	5063
13	0.00978	72.4	7403
14	0.00814	48.4	5946
17	0.00928	34.6	3728
19	0.01009	49.7	4926
20	0.00981	52.5	5352

Average stress = 5145 psi

Contact angle = 118°

Run No. 29 Gold-Oxygen, 1200° C, 1:02 hrs.

Sample No.	Area	Load	Stress
1	0.01096	50.8	4635
4	0.00884	42.9	4853
5	0.01102	57.0	51.72
6	0.0128	54.2	4805
7	0.00973	46.1	4738
8	0.00953	54.0	5666
9	0.01026	64.1	6248
10	0.00930	37.6	4043
11	0.01019	48.8	4789
12	0.01033	62.2	6021
13	0.01001	61.3	6104
14	0.00955	32.5	3403
16	0.01013	89.3	8815*
17	0.01000	56.1	5610
18	0.01021	43.8	4290
19	0.01176	91.9	7815
20	0.01052	61.0	5798

Average stress = 5459 psi

Contact angle = 116°

APPENDIX II

DISCUSSION OF DISPERSION FORCES

Brandner[20] has presented a development for the van der Waal dispersion forces acting on gold/sapphire adhesion couples. The equation for the force per unit area (a stress) is given as

$$(1) \qquad S = \frac{CN_o N_m}{6r^3}$$

where S = tensile stress the dispersion force will support.

C = the dispersion force constant for these materials.

N_o = the number of oxygen ions per unit volume in sapphire.

N_m = the number of gold atoms per unit volume.

r = the distance between the parallel surfaces of the adhesion couple.

In evaluating the constant terms of this expression a minor error in determining N_o was made. The calculation of N_o made previously was too large by a factor of 3. The incorrect value was later used to estimate the separation distance r_m at which the maximum forces occur. The method which was used to make the estimate of r_m does not give a reasonable result when the correct values from the dispersion force equation are used.

An alternate method to estimate this distance is as follows. Assume that the equilibrium spacing r_e is given by a hard sphere

model formed by a close packed plane of oxygen ions with gold atoms resting above the centroids of the oxygen ion equalateral triangles. This geometry gives

$$(2) \qquad r_e = \left[(r_o + r_{au})^2 - a^2 \right]^{1/2}$$

where $r_o = 1.37$ Å oxygen ion radius

$r_{au} = 1.44$ Å gold atom radius

$a = 2/3 \sqrt{3}\, r_o$

thus $r_e = 2.32$ Å

Further assume that the atoms are bound together by a Lennard-Jones type potential.

$$(3) \qquad E = -Ar^{-6} + Br^{-12}$$

The attraction term in equation (3) has the same exponent as is used in the development of the dispersion force equation. The repulsion term has been used in this form for convenience; however, an exponential term appears to be more correct. Taking the derivative of E with respect to r and noting

$$(4) \qquad \frac{d}{dr}(E)\Big|_{r=r_e} = -F = 6Ar_e^{-7} - 12Br_e^{-13} = 0$$

and

$$(5) \qquad Ar_e^{-7} = 2Br_e^{-13}$$

Taking the derivative of the force F with respect to r and noting

$$(6) \qquad \frac{d}{dr}(F)\Big|_{r=r_m} = \frac{d}{dr}\left[-\frac{dE}{dr}\right]\Big|_{r=r_m}$$

$$= 6\cdot 7\ Ar_m^{-8} - 12\cdot 13\ Br_m^{-14}$$

$$= 0$$

and

$$(7) \qquad 7Ar_m^{-8} = 26Br_m^{-14}$$

Taking the ratio of equations (5) and (7) and simplifying

$$(8) \qquad r_m = r_e \left[\frac{13}{7}\right]^{1/6} = 2.57\ \text{Å}$$

Brandner used 2.5 Å previously, and since this is close to the result obtained here, the same value will be used in this paper also.

BIBLIOGRAPHY

1. Lester, G. R., "Contact Angles of Liquids at Deformable Solid Surfaces", J. Colloid. Sci., Vol. 16, (1961), pp. 315-326.

2. Bondi, A., "The Spreading of Liquid Metals on Solid Surfaces; Surface Chemistry of High-Energy Substances", Chem. Revs., Vol. 52, No. 2 (1953), pp. 417-458.

3. Pask, J. A., and R. M. Fulrath, "Fundamentals of Glass-to-Metal Bonding: VIII, Nature of Wetting and Adherence", J. Amer. Ceram. Society, Vol. 45, No. 12, (1962), pp. 592-596.

4. Sutton, W. H., "Wetting and Adherence of Ni/Ni-Alloys to Sapphire", U. S. Dept. of Commerce Report, AD-600 995 (1964).

5. Kurkjian, C. R., and W. D. Kingery, "Surface Tension at Elevated Temperatures: III Effect of Cr, In, Sn, and Ti on Liquid Nickel Surface Tension and Interfacial Energy with Al_2O_3", J. Phys. Chem., Vol. 60, No. 7 (1956), pp. 961-963.

6. Armstrong, W. M., A. C. D. Chaklader, and J. F. Clarke, "Interface Reactions Between Metals and Ceramics: I Sapphire-Nickel Alloys", J. Am. Ceram. Soc., Vol. 45, No. 3 (1962), pp. 115-118.

7. Van Vlack, L. H., "The Metal-Ceramic Boundary", Metals Engineering Quarterly, ASM, Nov., 1965, pp. 7-12.

8. Mattox, D. M., "Interface Formation and the Adhesion of Thin Films", Sandia Corporation Monograph No. SC-R-65-852, January, 1965.

9. Ehrlich, G., "Atomistics of Metal Surfaces", SCI Monograph No. 28, Staples Printers Ltd., (1968), pp. 13-38.

10. Paulson, G. G., "Adhesion of Gold Thin Films to Glass Substrates", Ceramic Bulletin, Vol. 47, No. 4, (1968), pp. 374.

11. Mattox, D. M., "Influence of Oxygen on the Adherence of Gold Films to Oxide Substrates", J. App. Phys., Vol. 37, No. 9 (1966), pp. 3613-3615.

12. Dunning, W. J., "Theoretical Aspects of Adhesion", J. Oil and Color Chem. Assoc., Vol. 48, No. 10, (1965), pp. 509-519.

BIBLIOGRAPHY (cont'd)

13. Sharpe, L. H., and H. Schonhorn, "Surface Energetics, Adhesion, and Adhesive Joints", Advances in Chemistry Series, No. 43, Amer. Chem. Soc., (1964), pp. 189-201.

14. Moore, D. G., and H. R. Thornton, "Effect of Oxygen on the Bonding of Gold to Fused Silica", Journal of Research of the National Bureau of Standards, Vol. 62, No. 3 (1959), pp. 127-135.

15. Benjamin, P., and C. Weaver, "Adhesion of Metal Film to Glass", Proc. Roy. Soc., Vol. 254 (1960), pp. 177-183.

16. Benjamin, P., and C. Weaver, "The Adhesion of Evaporated Metal Films on Glass", Proc. Roy. Soc., A, Vol. 261, (1961), pp. 516-531.

17. Helgesson, C. I., "Ceramic-to-Metal Bonding", Boston Tech. Publishers, Inc., (1968).

18. Benjamin, P., and C. Weaver, "The Adhesion of Metals to Crystal Faces", Proc. Roy. Soc., A, Vol. 274 (1963), pp. 267-273.

19. Haq, K. E., and K. H. Behrndt, and I. Kobin, "Adhesion Mechanism of Gold-Underlayer Film Combinations to Oxide Substrates", J. Vac. Sci. and Tech., Vol. 6, No. 1, (1969), pp. 148-152.

20. Brandner, J. L., "The Adhesion of Gold to Aluminum Oxide", Masters Thesis, Lehigh University, Bethleham, Pa. (1969).

21. Benjamin, P., and Weaver, C., "Condensation Energies for Metals on Glass and Other Substrates", Proc. Roy. Soc., A, Vol. 252, (1959), pp. 418-430.

22. Chang, C. C., "LEED Studies of the (0001) Face of Alpha-Alumina", J. App. Phys., Vol. 39, No. 12, (1968), pp. 5570-5573.

23. Weaver, C., "The Adhesion of Metal Films to Surfaces", Chemistry and Industry, Feb. 27, 1965, pp. 370-373.

24. Paulson, G. G., "Interface Phenomena and Adhesion of Gold This Films on Glass", Doctors Thesis, University of Illinois, (1969).

BIBLIOGRAPHY (cont'd)

25. Pauling, L. and E. B. Wilson, "Introduction to Quantum Mechanics", McGraw-Hill Book Co. Inc., (1935), pp. 383-388.

26. Strong, J., "On the Cleaning of Surfaces", Rev. Sci. Instr., Vol. 6, (1935), pp. 97.

27. Benjamin, and C. Weaver, "Measurement of Adhesion of Thin Films", Proc. Roy. Soc., A, Vol. 254, (1960), pp. 163-176.

28. Belser, R. B., and M. D. Carither, "Reflective Coatings on Polymeric Substrates", A.S.D. Technical Report 61-151-2, (1961).

29. Peters, F. G., "Bond Strength of Metallic Films Deposited on Polycrystaline Garnets", Ceramic Bulletin, Vol. 48, No. 2, (1969), pp. 228-229.

30. Moses, S. T., and R. K. Witt, Industr. Eng. Chem., Vol. 41, (1949), pp. 2334.

31. Richardson, E. G., "Technical Aspects of Sound II", (1957), Elsevier.

32. Beams, J. W., and W. E. Walker, and H. S. Morton, "Mechanical Properties of Thin Films of Silver", Phys. Rev., Vol. 87, (1952), pp. 524.

33. Beams, J. W., and J. B. Breazeale, and W. L. Bart, Phys. Rev., Vol. 100, (1955), pp. 1657.

34. Beams, J. W., 43rd Ann. Proc. Amer. Electropl. Soc., (1956).

35. Oishi, Y., and W. D. Kingery, "Self-Diffusion of Oxygen in Single Crystal and Polycrystalline Aluminum Oxide", J. Chem. Phys., Vol. 33, No. 2, (1960), pp. 480-486.

36. Rossing, B. R., "Adherence of Nickel-Oxygen Alloys to Alumina", Ceramic Bulletin, Vol. 49, No. 4, (1970), pp. 401.

37. Clark, D., and T. Dickinson, and W. N. Mair, "The Interaction of Oxygen and Hot Gold, Part 2, Electron-Diffraction, X-Ray, and Electrochemical Studies", Trans. Faraday Soc., Vol. 55, (1959), pp. 1937-1946.

BIBLIOGRAPHY (cont'd)

38. Shishakov, N. A., "On The Oxidation of Gold", J. Phys. Chem., Vol. 64, (1960), pp. 1580.

39. Shishakov, N. A., and V. V. Andreewa, "Oxide Films on Metals", Acad. Sci. URSS, Moscow, (1959).

40. Clark, D., and T. Dickinson, and W. N. Mair, "On the Oxidation of Gold", J. Phys. Chem., Vol. 65, (1961), pp. 1470.

41. Kubaschewski, O., and B. E. Hopkins, "The Oxidation of Metals and Alloys", Academic Press Inc., (1962), pp. 2.

42. Meyer, D. T., "A Gold Surface Phase: Its Formation and Properties on Thin Films of Gold", Thin Solid Films, 2 (1968), Elsevier, pp. 27-42.

43. Weyl, W. A., "The Theoretical Basis of Adhesion", Proc. ASTM, (1946), pp. 1506-1516.

VITA

Leo Lawrence Radke, son of Gottfried and Tina Radke, was born January 2, 1933, in Logan County, North Dakota. He completed high school in Absarokee, Montana in 1950. He enrolled in the College of General Engineering at the University of Portland, Portland, Oregon in 1956, and graduated in 1960 with a BSGE.

In 1960 he was employed by the Western Electric Company as an engineer in the Defense Activities Division, where he worked on a wide scope of engineering assignments. In 1962 he was promoted to planning engineer, and in 1968 he was accepted as a candidate to the Western Electric Lehigh Master's Degree Program.